



HAL
open science

Climatic change and diet of the pre-Hispanic population of Gran Canaria (Canary Archipelago, Spain) during the Medieval Warm Period and Little Ice Age

Christophe Lécuyer, Jean Goedert, Johanne Klee, Thibault Clauzel, Pascale Richardin, François Fourel, Teresa Delgado-Darias, Verónica Alberto-Barroso, Javier Velasco-Vázquez, Juan Francisco Betancort, et al.

► To cite this version:

Christophe Lécuyer, Jean Goedert, Johanne Klee, Thibault Clauzel, Pascale Richardin, et al.. Climatic change and diet of the pre-Hispanic population of Gran Canaria (Canary Archipelago, Spain) during the Medieval Warm Period and Little Ice Age. *Journal of Archaeological Science*, 2021, 128, pp.105336. 10.1016/j.jas.2021.105336 . hal-03293366

HAL Id: hal-03293366

<https://hal.science/hal-03293366>

Submitted on 14 Feb 2023

HAL is a multi-disciplinary open access archive for the deposit and dissemination of scientific research documents, whether they are published or not. The documents may come from teaching and research institutions in France or abroad, or from public or private research centers.

L'archive ouverte pluridisciplinaire **HAL**, est destinée au dépôt et à la diffusion de documents scientifiques de niveau recherche, publiés ou non, émanant des établissements d'enseignement et de recherche français ou étrangers, des laboratoires publics ou privés.



Distributed under a Creative Commons Attribution - NonCommercial - NoDerivatives 4.0 International License

1 **Climatic change and diet of the pre-Hispanic population of Gran Canaria (Canary**
2 **Archipelago, Spain) during the Medieval Warm Period and Little Ice Age**

3
4 Christophe Lécuyer^{1,*}, Jean Goedert¹, Johanne Klee¹, Thibault Clauzel¹, Pascale Richardin^{2,**},
5 François Fourel³, Teresa Delgado-Darias⁴, Verónica Alberto-Barroso⁵, Javier Velasco-
6 Vázquez⁶, Juan Francisco Betancort⁷, Romain Amiot¹, Chloé Maréchal⁸ and Jean-Pierre
7 Flandrois⁹

8
9 ¹Univ Lyon, Univ Lyon 1, ENSL, CNRS, LGL-TPE, F-69622, Villeurbanne, France.
10 jean.goedert@protonmail.com. Johanne.Klee@gmail.com. Thibault.Clauzel@univ-lyon1.fr.
11 Romain.Amiot@univ-lyon1.fr. Christophe.Lecuyer@univ-lyon1.fr.

12 ²Centre de Recherche et de Restauration des Musées de France, Palais du Louvre, 75001 Paris, France.
13 pascale.richardin@culture.gouv.fr.

14 ³Plateforme d'écologie isotopique, LEHNA, UMR CNRS 5023, University of Lyon, France.
15 Francois.Fourel@univ-lyon1.fr

16 ⁴El Museo Canario, Doctor Verneau, 2, Vegueta 35001, Las Palmas de Gran Canaria, Spain.
17 tdelgado@elmuseocanario.com

18 ⁵Tibicena Arqueología y Patrimonio. Las Palmas de Gran Canaria, Spain. veroalberto1@gmail.com

19 ⁶Servicio de Patrimonio Histórico, Cabildo de Gran Canaria, Spain. jvelascov@grancanaria.es

20 ⁷Departamento de Biología, Universidad de Las Palmas de Gran Canaria, Las Palmas de Gran Canaria, Spain.
21 juanbetancort@gmail.com

22 ⁸Observatoire des Sciences de l'Univers de Lyon, France. Chloe.Marechal-Chenevier@univ-lyon1.fr

23 ⁹LBBE, UMR CNRS 5558, Université de Lyon 1 and Faculté de Médecine Lyon-Sud, France. Jean-
24 Pierre.Flandrois@univ-lyon1.fr

25 *also at Institut Universitaire de France. clecuyer@univ-lyon1.fr

26 ** Préhistoire & Technologie (PRETECH), UMR CNRS 7055, Paris-Nanterre University, Nanterre, France.

27

28

29
30
31
32
33
34
35
36
37
38
39
40
41
42
43
44
45
46
47
48
49
50
51
52
53

Abstract – The hard and soft tissue remains of a pre-Hispanic population of the Gran Canaria Island at six different archaeological localities were studied using ^{14}C dating and stable isotope compositions. Radiocarbon dating indicates island occupation ranging from the beginning of the 7th to the mid-14th century. We analyzed the oxygen isotope compositions of apatite phosphate bones of some pre-Hispanic individuals. The oxygen isotope compositions of meteoric water ($\delta^{18}\text{O}_w$) show a significant decrease from -2.1 ± 1.5 to -4.4 ± 1.2 ‰ (VSMOW) from the Medieval Warm Period (MWP) to the Little Ice Age (LIA). This is interpreted to reflect a decrease in air temperature by about $5\pm 3^\circ\text{C}$. Archaeological data along with $\delta^{13}\text{C}$, $\delta^{15}\text{N}$ and $\delta^{34}\text{S}$ values of soft tissue indicate that the pre-Hispanic population from Gran Canaria relied on agriculture throughout the 7th to mid-14th century. However, a significant contribution of seafood to the diet of the pre-Hispanic population is observed at archaeological sites located close to the shore. These results suggest cultural resilience in the pre-Hispanic population of Gran Canaria, reflected in the relative constancy of their diet in light of climate change.

Keywords: pre-Hispanic population; Gran Canaria; climate change; diet; stable isotopes; medieval warm period; little ice age

54

55 **1. Introduction**

56 Since the beginning of the Holocene (Moberg et al., 2005; Marsicek et al., 2018),
57 including the last millenium (e.g. Soon and Baliunas, 2003), significant warming and cooling
58 events have been documented throughout the Holocene. Climatic variations may impact
59 civilizations through disease, starvation, migration, revolution, and wars, along with the long-
60 term risk of eroding their cultural identity (e.g. DeMenocal, 2001; Prentice, 2009; Büntgen et
61 al. 2011; 2016).

62 Holocene climatic change recorded for the past 5,000 years has been attributed to
63 collapses of civilizations such as the Akkadian of Mesopotamia (about 2200 BCE), the
64 Mayan of the Yucatán Peninsula (about 1500 AD), the pre-Inca Tiwanaku of the Bolivian–
65 Peruvian Altiplano (about 1000 AD; DeMenocal, 2001), and the Norse from Greenland
66 (around 1450-1500 AD; Arneborg et al., 2002; Dugmore et al. 2007; D’Andrea et al., 2011).
67 In contrast, despite experiencing severe drought for several millennia, long-term resilience
68 has been documented for the Ancient Egyptians (Touzeau et al., 2013).

69 The main climatic changes of the last two millennia are the Medieval Warm Period
70 (MWP) from about 1000 to about 1300 AD (Le Roy Ladurie, 1971), and the Little Ice Age
71 (LIA) from about 1300 to about 1850 AD (Le Roy Ladurie, 1967). In Europe, the LIA was
72 characterized by colder climates, early snow events, frequent storms of high magnitude and
73 recurrent floods. The LIA was a period of repeating cooling events, each characterized by low
74 sunspot activity, decreased solar irradiance and magnetism (e.g. Easterbrook, 2016). In
75 Europe, many societies showed increased vulnerability and lowered resilience during periods
76 of extreme storm activity impacting the English, Dutch, Danish and German coasts (e.g.
77 Lamb, 1980; Athimon and Maanan, 2018).

78 A number of causes have been proposed to explain the peculiar climatic conditions of the
79 LIA. Several authors (DeMenocal et al, 2000; Maslin et al., 2001; Paasche and Bakke, 2010;
80 Henke et al., 2017; Ilyashuk et al., 2019; Fang et al., 2019) suggested that the LIA was
81 initiated by a major shift in atmospheric circulation patterns of the Intertropical Convergence
82 Zone (ITCZ), the West African Monsoon (WAM), the Northern Annular Mode (NAM) also
83 called Arctic Oscillation (AO), the North Atlantic Oscillation (NAO) and the El Niño–
84 Southern Oscillation (ENSO). Those atmospheric perturbations were documented altogether
85 around 1400 AD at a time of reduced solar activity (Spörer, 1450–1550 AD; Maunder, 1645–
86 1715 AD and Dalton, 1790–1820 AD), lower sunspot occurrence (Paasche and Bakke, 2010;
87 Easterbrook, 2016; Owens et al., 2017; Zharkova et al., 2019), as well as a decrease in
88 greenhouse gas contents (CO₂ and CH₄), which remained low until about 1800 AD
89 (Robertson et al., 2001; Siegenthaler et al., 2005; Macfarling Meure et al., 2006).

90 Volcanic eruptions are known to have a notable impact on climate because they release
91 dust clouds and sulfur dioxide into the atmosphere as exemplified by the Laki eruption on
92 Iceland (Thordarson and Self, 1993). Another consequence of volcanic eruptions, besides a
93 cooling of the atmosphere, is a weakening of westerlies in the following decade (Shindell et
94 al., 2003). Such catastrophic events are considered key roles in the disturbed and colder
95 climatic conditions that prevailed with the onset of the LIA (e.g. Miller et al., 2012;
96 Brönnimann et al., 2019).

97 Another recent and different explanation for colder climatic conditions during the 16th
98 century, is human-induced perturbation of the carbon cycle with the European conquest of the
99 Americas in 1492. Indeed, Koch et al. (2019) proposed that the “Great Dying” of indigenous
100 populations of the Americas resulted in abandoned sites. Subsequent growth of vegetation on
101 the vacated land surface, covering about 5.6×10^5 km², extracted a substantial amount of

102 carbon dioxide from the atmosphere resulting in a decrease of air temperature (Koch et al.,
103 2019).

104 Most records of LIA climatic conditions were obtained from high-latitude archives of the
105 Northern Hemisphere, particularly the North Atlantic region and Europe (Mann et al., 2009).
106 Therefore, it was originally thought that the LIA mainly, or only, impacted the mid- to high-
107 latitudes (Lane et al., 2011), and consequently the populations living in those areas.
108 Nonetheless, climatic perturbations contemporaneous to the LIA were also recorded at low
109 latitudes in the Caribbean Islands (Lane et al., 2011), in South America (Brown and Johnson,
110 2005), in equatorial Africa (Verschuren et al., 2000; Russel and Jonhson 2007), in East Africa
111 (Russell et al., 2007), in tropical southeast Africa (Johnson et al., 2001; Brown and Jonhson,
112 2005), in South Africa (Huffman, 1996; Tyson et al., 2000; Holmgren et al., 2001) and in
113 tropical northwest Africa (DeMenocal et al., 2000) (Supplementary Figure 1; Supplementary
114 Table 1).

115 Located in the eastern part of the central Atlantic Ocean, Gran Canaria is one of the
116 seven main islands of the Canary Archipelago which is situated close to the Sahara coast (\approx
117 200 km), ranging from 27° to 29° N latitude (Figure 1). Although many uncertainties remain
118 so far, the Canary Archipelago was colonized by people of North African origin at the
119 beginning of the first millennium AD (Velasco-Vázquez et al, 2019). This hypothesis has
120 been reinforced by genetic studies (Pinto et al., 1996; Rando et al., 1999; Maca-Meyer et al.,
121 2004; Arnaiz-Villena et al., 2015; Rodríguez-Varela et al., 2017). Strong cultural differences
122 exist between the archaeological remains of the different islands. For example, remains from
123 Gran Canaria tend to support the existence of a proto–urban society, adapted to the specific
124 geoclimatic conditions of the island marked by an abrupt landscape with central mountains
125 reaching nearly 2000 m.

126 Human resilience to past climate changes may be approached through the lens of the
127 cultural heritage record, which includes the relative steadiness of diet composition. In order to
128 test such hypothesis, we analyzed the isotopic compositions of the pre-Hispanic people living
129 on Gran Canaria. Oxygen isotope ratios of human bones were measured in order to estimate
130 changes in the composition of meteoric waters that constitutes a proxy of mean annual air
131 temperature. Bone collagen was analyzed for its stable isotope compositions ($\delta^{13}\text{C}$, $\delta^{15}\text{N}$ and
132 $\delta^{34}\text{S}$) in order to estimate the diet, especially to distinguish between dietary products derived
133 from inland agriculture, cattle raising, and by fishing. In addition, a large dataset of new ^{14}C
134 dates was obtained from the human collagen to provide a timeline whether or not climate
135 change, which took place during the transition between the MWP and the LIA, had an impact
136 on the diet of the inhabitants of the island of Gran Canaria.

137

138 **2. Pre-Hispanic people from Gran Canaria**

139 The Canary Islands were originally settled by people from North Africa belonging to
140 the Amazigh sphere. Cultural material and linguistic evidence revealed this origin, and was
141 confirmed by genetic data (Fregel et al., 2009; Guatelli-Steinberg et al., 2001; Maca-Meyer et
142 al., 2004). However, the exact geographic area of North Africa where the colonizers came
143 from and the precise processes of colonization remain unclear. According to the latest
144 radiocarbon studies, those people probably arrived around the beginning of the first
145 millennium AD (Velasco-Vázquez et al., 2019). The Amazigh settlers introduced
146 domesticated plants (barley, wheat, fig, and some pulses) and livestock of goats, sheep and
147 pigs, ensuring a steady food supply.

148 Once the Canary Archipelago was settled, it remained relatively isolated although
149 there is evidence of later arrivals once again linked to the Amazigh cultural context.
150 Paleogenomic analysis revealed that some islands experienced a single colonization event

151 while others, such as Lanzarote, Fuerteventura and Gran Canaria, experienced at least a
152 second event (Fregel et al., 2015; 2019; Ordoñez et al., 2017; Santos et al., 2010). Each
153 insular population developed a specific economy and social structure conditioned by the
154 natural peculiarities of each territory. This changed once Europeans discovered the
155 archipelago in the 13th to 14th centuries AD. In the late 15th century, the Crown of Castile
156 conquered the islands leading to extirpation of the indigenous culture.

157 The earlier population on Gran Canaria, known as ancient Canarians, is assigned to the
158 3rd-4th century AD (Alberto et al., 2019; Velasco-Vázquez et al., 2019). Archaeological
159 investigations revealed a complex development with profound changes throughout their
160 historical evolution. In the early stages of settlement, these people exhibit an agro-pastoralist
161 organization, linked to the use of caves and with a major role for livestock in its production
162 base. In this first stage, the interpersonal relationship system suggests a preponderance of
163 group behaviour in which the sense of community prevailed, without excessive distinction in
164 the social consideration of people. From the 6th-7th centuries AD, this dynamic came into
165 conflict with the role of agriculture, as a support for the economic system and as the
166 foundation of its organizational system.

167 From the 11th century AD, the preceding situation of rupture and imbalance was fully
168 consolidated in favour of a hierarchical organization agricultural in nature. Archaeological
169 data indicate a significant demographic increase, as well as the flourishing of stone house
170 settlements located in the fertile plains of the mouth of the great ravines and somewhat later in
171 the coastal areas. This last stage of development was characterized by a stratified society, with
172 agriculture being the most important economic activity, based on barley (*Hordeum*
173 *vulgare* ssp.), wheat (*Triticum aestivum/durum*), and figs (*Ficus carica*) as the most common
174 species found in archaeological sites. In addition, wild fruits such as dates of Canarian palm
175 (*Phoenix canariensis*) were gathered by the indigenous population, incorporating them into

176 their diet. (Morales, 2019; Morales et al., 2014; Hagenblad et al., 2017). A number of
177 communal fortified granaries were carved into volcanic tuff rock to store the crop. Vegetarian
178 diet was complemented with cattle products (Alberto et al., 2017). Fishing was also practiced
179 as testified by fish remains of *Sparisoma cretense*, *Clupeidae*, *Engraulis encrasicolus*
180 (Rodríguez Santana, 1996) and shells of *Osilinus* and *Patella* being frequently recovered from
181 archaeological records of villages next to the sea.

182 Several results of paleodiet analyses of human bones and teeth support the above
183 considerations and the importance of cultivated plants in the diet of the ancient Canarios (cf.
184 trace element patterns, stable isotope compositions of soft tissues, high prevalence of dental
185 caries or high proportion of osteopenia; Velasco-Vázquez et al., 2000; González-Reimers et
186 al., 2002; Delgado-Darias et al., 2005; Arnay-de-la-Rosa et al. 2010). The analysis of
187 enthesal changes in bones of ancient Canarios is consistent with a dominant position of
188 agriculture in the daily activity of pre-Hispanic people in Gran Canaria (Santana Cabrera et
189 al., 2012). This economic structure allowed Gran Canaria to support a high population density
190 in pre-Hispanic times. According to archaeological data and ethnohistorical texts, nearly
191 30,000 to 50,000 Canarios inhabited the island when Europeans landed.

192

193 **3. Material and Methods**

194 *3.1. Archaeological sites*

195 Guayadeque is a large ravine in the southeast mountains of the island (Figure 1).
196 Several villages are spread throughout the ravine, comprising natural and artificial caves for
197 dwelling and collective granaries revealing extensive agricultural activity. Food remains such
198 as seeds and fruits of the diet of the pre-Hispanic inhabitants have been recovered from these
199 storage areas. Next to these domestic sites, several cemeteries were also established in caves.
200 They consist of collective burials in which individuals were deposited wrapped in shrouds

201 made of rush fibres or animal skins, following the common mortuary practices of the ancient
202 Canarians (Alberto et al., 2014). The environmental conditions in the caves led to the
203 desiccation of the human soft tissue of some individuals, as well as that of their shrouds, in
204 the same way it occurs with domestic plants, insects and other organic artefacts in domestic
205 caves (Henríquez-Valido et al., 2019; Vidal-Matutano et al., 2020). Absolute dating of some
206 human skeletal remains (Velasco-Vázquez et al., 2019) range from 1550±30 BP to 768±25
207 BP.

208 Acusa is located inland on the western part of the island (Figure 1), placed on a
209 volcanic plateau surrounded by cliffs. It can be considered as a strategic site regarding the
210 space available for crops, cattle raising, fodder storage and water supply. This is a large
211 settlement consisting of natural and artificial cave-rooms, communal granaries and collective
212 burial sites. Some of these funerary caves were excavated at the beginning of the 20th century,
213 recovering human remains shrouded in animal skins and rush fibres, together with some
214 funerary wood boards where the corpses lay. As in Guayadeque valley, the excellent
215 preservation of these remains was propitiated by the natural environmental conditions of the
216 caves. Radiocarbon dating of these human remains ranges from 1540±30 BP to 1230±30 BP
217 (Delgado-Darias, 2020; Velasco-Vázquez et al., 2019).

218 Andén del Tabacalete or Roque Camello is one of the three peaks raised in the
219 volcanic basin of Tejeda, in the mountainous central area of the island. This place hosts
220 abundant vestiges of aboriginal settlements with more than a hundred of natural and artificial
221 caves for housing, long-term storage of food products and necropolises. One of these
222 cemeteries is located in the south face of the Andén del Tabacalete peak, near its top,
223 consisting of small collective caves. Some of them were excavated in the 30s and 40s,
224 recovering human remains and fragments of rush fibres (Delgado-Darias, 2009).

225 El Agujero-La Guancha is referred to a stone house village and a salient necropolis
226 located in the northwestern coast of the island. The cemetery comprises individual stone cists
227 and oval burial pits dug directly into the ground, arranged in seven units that show different
228 dimensions and complexity. Each of them is defined by stone structures that organize and
229 divide the burial space, denoting a hierarchical layout. Two of these structures were dug in the
230 30s, recovering the remains of 6 and 58 individuals. According to radiocarbon dating obtained
231 so far, the necropolis was in use between 910±40 BP and 530±40 BP (Santana Cabrera et al.,
232 2012).

233 Lomo Maspalomas, located in the southernmost part of the island (Figure 1), was a
234 large necropolis of around 2000 m² with 142 graves in oval burial pits and, to a lesser extent,
235 in cists. Most of them were individual tombs, arranged into groups (Alberto and Velasco,
236 2009-2010). This site was probably highly strategic for the inhabitants of the southernmost
237 part of the island, with close vicinity to the coast and the mouth of the Fataga ravine.
238 Radiocarbon dating places the age of the necropolis from 820±40 BP to 440±30 BP (Santana
239 Cabrera et al., 2012; Velasco-Vázquez et al., 2019).

240 El Hormiguero, located in the northernmost part of the island (Figure 1), is another
241 coastal cemetery consisting of small collective funerary caves. In the late 60s, two of them
242 caves (number 4 and 5) were excavated. Skeletal remains of 12 and 4 individuals were
243 recovered from each one and rush fibres from the shrouds that covered the bodies. Stone walls
244 closing the entrance of both caves were documented and also divided the internal space of
245 cave number 5 (Navarro Mederos, 1979). Radiocarbon dating available from human bone
246 samples (cave 4) places this cemetery at about 950±30 BP (Santana Cabrera et al., 2012).

247 Different funerary practices following a marked diachronic order can be distinguished
248 among the ancient Canarians. Thus, collective funerary caves spread across the island along
249 the whole pre-Hispanic period, characterized by a close link to dwelling places. Between the

250 7th and 11th centuries, the ancient Canarians built large tumular necropolises in lava flows and
251 rocky areas. From 11th-12th centuries up to the moment of the Castilian Conquest (1483), they
252 buried their dead in cemeteries consisting of pits and cists, most of them located on the
253 coastline, and close to the villages.

254 These changes in funerary traditions over time have been recently related to internal
255 processes of social and economic changes, in which interpersonal relationships became more
256 asymmetrical, without ruling out possible punctual arrivals from North Africa that could
257 introduce new cultural habits (Alberto et al., 2019; Fregel et al., 2019). Despite the different
258 typology, organization and dimensions of the cemeteries, the treatment of the corpses
259 (covered by either a shroud of animal skins or rush fibres) and the arrangement of the bodies
260 in the tombs (laid down in an extended supine) did not change with time.

261

262 3.2. *Sampling*

263 3.2.1. *Hard and soft tissues from human, cattle and food remains*

264 All the samples analyzed in this study came from the anthropological collection of El
265 Museo Canario, Las Palmas, Spain. Human and cattle remains were found in six
266 archaeological sites (Figure 1), which are from north to south 1) Agujero-La Guancha, 2)
267 Hormiguero, 3) Acusa, 4) Tejeda, 5) Barranco de Guayadeque, and 6) Maspalomas. The
268 sampling performed on human and animal remains for ¹⁴C dating (bone collagen), the oxygen
269 isotope compositions of the cortical part of the bone or tooth phosphate, and the carbon,
270 nitrogen and sulfur isotope compositions of bone and soft tissues are given in Supplementary
271 Tables 2, 3 and 4, respectively. The location and nomenclature of skeletal bones and teeth as
272 well as the types of organic matter (bone collagen, skin, tendon, animal leather) we analyzed
273 are also given in Supplementary Tables 3 and 4. In addition, a few remains of food (fig, wheat
274 and barley seeds) stored in the caves were also analyzed for their carbon, nitrogen and sulfur

275 isotope compositions (Supplementary Table 4) as well as of the rush fibres (Supplementary
276 Table 4) used for wrapping of the human bodies.

277

278 *3.2.2. Present-day fresh and marine water samples*

279 Three sea surface waters (GC-1 to GC-3) and eleven fresh water samples (GC-4 to
280 GC-14) were sampled in different spots of Gran Canaria. Location and altitude relative to sea
281 level are given in Figure 1 and Supplementary Table 5. Seawater was sampled along the
282 northern and southern coasts at a depth range of 1 to 2 meters below sea level. Fresh waters
283 are either flowing waters in springs, irrigation ditches or surficial wells feed by rain. One
284 sample (GC-14) corresponds to water sampled in a natural pond (Supplementary Table 5).

285

286 *3.3. Radiocarbon dating and stable isotopes analyses*

287 All methods for extraction of soluble collagen, radiocarbon dating, hydrogen and
288 oxygen isotope analyses of present-day waters, oxygen isotope analysis of phosphate as well
289 as carbon, nitrogen and sulfur isotope analysis of collagen are available in Supplementary
290 Material (Methods).

291

292 **4. Results**

293 *4.1. ¹⁴C dating*

294 Twenty-nine calibrated ¹⁴C dates obtained from human and cattle bone collagen range
295 from 553-648 cal AD (95.4%) to 1310-1431 cal AD (95.4%) (Supplementary Table 2). These
296 dates encompass the transition between the Medieval Warm Period (MWP) (highlighted in
297 grey in Supplementary Table 2) and the beginning of the Little Ice Age (LIA). Ranges of
298 calibrated dates obtained for each studied archaeological site are reported in Figure 1. Here,

299 we emphasize that the two archaeological sites (Agujero, Maspalomas) occupied by pre-
300 Hispanic populations during the LIA are located along the coast.

301

302 *4.2. Hydrogen and oxygen isotope compositions of present-day waters*

303 Waters from Gran Canaria were collected from 27th to 29th August 2018. Sea surface
304 waters have $\delta^{18}\text{O}_{\text{sw}}$ of 0.97‰, 0.83‰ and 0.87‰ (VSMOW) with an average value of
305 0.89 ± 0.07 ‰ (Supplementary Table 5). This mean value compares well with data published
306 by Clauzel et al. (2020) for the coastal sea surface waters of Lanzarote ($\delta^{18}\text{O} = 1.09$ ‰) and
307 Fuerteventura ($\delta^{18}\text{O} = 1.08$ ‰), the easternmost islands of the archipelago (Figure 1). Such
308 oxygen isotope compositions are higher than the SMOW reference reflect a tropical
309 environment where the ratio between evaporation and precipitation is higher than one. Indeed,
310 the Köppen-Geiger climate subtype climate mode (Kottek et al., 2006) for the island is rated
311 as Bwh (Tropical and Subtropical Desert Climate) with a mean annual air temperature
312 (MAAT) of 20.7°C, the warmest month is August ($T = 24.2$ °C) and the coldest month is
313 January ($T = 17.6$ °C). Mean annual precipitation (MAP) is close to 135 mm (National Center
314 for Atmospheric Research).

315 Fresh waters have $\delta^2\text{H}$ and $\delta^{18}\text{O}$ values ranging from -23.8 to 1.7 and from -4.93 to -
316 0.03 ‰ (VSMOW), respectively. Both $\delta^2\text{H}$ and $\delta^{18}\text{O}$ values define a line whose slope ‘S’ is
317 5.54 ± 0.52 with an intercept ‘d’ of 5.42 ± 1.95 (Figure 2), which reflects the local meteoric
318 water line (LMWL). However, water sample GC-6 suffered significant evaporation while
319 resting in a pond, as testified by its high $\delta^2\text{H}$ and $\delta^{18}\text{O}$ values close to the SMOW values
320 (Figure 2). Therefore, it was excluded from the dataset before computing the LMWL (Figure
321 2), for which the linear correlation is highly significant according to the Pearson’s product
322 moment correlation ($p = 5.4 \times 10^{-6}$ for the null hypothesis $H_0 =$ no correlation between the two
323 variables). Compared to the Global Meteoric Water Line (GMWL), as defined by Dansgaard

324 (1964), both slope (as low as 5) and intercept lower than those of the GMWL ($S = 8$; $d = 10$;
325 Figure 2) constitute parameters commonly documented in tropical islands (Dansgaard, 1964).

326 An altitude effect upon the stable isotope compositions of meteoric waters ($\delta^{18}\text{O}_{\text{mw}}$) is
327 also observed in Gran Canaria (Figure 3). For example, $\delta^{18}\text{O}_{\text{mw}}$ values (‰ VSMOW)
328 negatively correlate with altitude (in meters a.s.l.). The slope of the line of best fit
329 corresponds to a decrease in $\delta^{18}\text{O}_{\text{mw}}$ by 1.97 ± 0.91 ‰ per 1,000 m ($R = 0.61$). Even if
330 significant (Pearson's product moment correlation test: $p = 0.06$ for the null hypothesis $H_0 =$
331 no correlation between the two variables), the rather weak correlation results from the sample
332 strategy. Indeed, water was collected from springs, i.e. where the water table intersects the
333 Earth's surface, which implies that the altitude of catchment is most likely higher in several
334 cases. The gradient we calculated fall in the range of those documented by Gonfiantini et al.
335 (2001) who established oxygen isotope gradients for meteoric waters with altitude (per 1,000
336 m) of -1.56 ± 0.05 ‰ for Mount Cameroon, Africa, and of -2.39 ± 0.15 ‰ for two Altiplano-
337 Amazon transects through Bolivia.

338

339 4.3. Oxygen isotope analysis of skeletal apatite phosphate

340 Oxygen isotope compositions of apatite phosphate ($\delta^{18}\text{O}_{\text{p}}$) have been determined on
341 skeletal remains of pre-Hispanic populations (Supplementary Table 3). As a whole, their
342 $\delta^{18}\text{O}_{\text{p}}$ values range from 17.6‰ to 21.8‰ with a mean of 19.3 ± 0.9 ‰ (VSMOW). Range and
343 mean of $\delta^{18}\text{O}_{\text{p}}$ values (VSMOW) obtained for each studied archaeological site are represented
344 in Figure1. It is worthy to mention that there is quite large variation in $\delta^{18}\text{O}_{\text{p}}$ values of
345 individuals at any given site. Such pattern could be the result of human mobility within the
346 island of Gran Canaria as well as the record of an interannual variability in the oxygen isotope
347 composition of precipitation.

348 In a first step, the oxygen isotope compositions of human skeletal remains have been
349 converted into $\delta^{18}\text{O}$ of drinking water (assumed to be a good approximation of precipitation in
350 the island) according to the equation determined by Daux et al. (2008). In a second step, the
351 calculated $\delta^{18}\text{O}_{\text{mw}}$ were corrected for the altitude effect according to a gradient of -
352 $1.97\pm 0.91\text{‰}$ per 1,000 m (§ section 4.2), to an altitude close to sea level. Those corrected
353 $\delta^{18}\text{O}_{\text{mw}}$ are reported in Supplementary Table 3 and Figure 4 for further interpretation and
354 discussion.

355 We also analyzed a tooth of a parrotfish (*Sparisoma cretense*) from Bocabarranco,
356 Gáldar, Gran Canaria, (Supplementary Table 3), a stone house village dated to the 13th
357 century (Velasco-Vázquez et al., 2019). This tooth sample provided a $\delta^{18}\text{O}_{\text{p}}$ of 22.1‰
358 (VSMOW). Considering that sea-level and the coastal $\delta^{18}\text{O}_{\text{sw}}$ ($0.89\pm 0.07\text{‰}$) remained
359 constant for the last millenia, a seawater temperature of $22\pm 1^\circ\text{C}$ has been estimated using the
360 oxygen isotope fractionation equation determined by Lécuyer et al. (2013).

361

362 4.4. Carbon, nitrogen and sulfur isotope ratios of human bone collagen

363 Bone collagen samples have a carbon amount of between 33.0% and 42.6%, with an
364 average %C of $40.6\pm 2.0\%$ and a nitrogen amount of between 12.3% and 15.9%, with an
365 average %N of $15.4\pm 0.8\%$ (Supplementary Table 4). These values are higher than the
366 thresholds defined by Van Klinken (1999) (%C > 30% and %N > 10%) to assess the
367 preservation of collagen. C/N ratios range from 3.03 to 3.37 with a mean of 3.09 ± 0.09
368 (Supplementary Table 4). These values, although a little low, lie in the range recommended
369 by DeNiro (1985) for well-preserved collagen (2.9 to 3.6) from archaeological human
370 remains. Carbon, nitrogen and sulfur isotope ratios were measured on four categories of
371 archaeological artefacts (Supplementary Table 4), which are 1) food remains, 2) rush fibres,
372 and animal leather wrapping of human mummies, 3) cattle bone collagen, and 4) human bone

373 collagen and other soft tissues such as skin and tendon. As a whole, these artefacts have $\delta^{13}\text{C}$,
374 $\delta^{15}\text{N}$ and $\delta^{34}\text{S}$ values ranging from -24.6‰ to -18.4‰, 4.0‰ to 13.0‰, and 14.0‰ to 21.1‰,
375 respectively. A few striking points, however, are underlined:

- 376 - In the case of Mummy 6, we notice that soft tissue is depleted in ^{13}C by 1.7‰ and
377 enriched in ^{34}S by 3.7‰ relative to bone collagen (Supplementary Table 4). Isotopic
378 differences between bone collagen and soft tissues have been studied on archeological
379 and modern human individuals (O'Connell et al., 1999; 2001). The enrichment of bone
380 collagen in ^{13}C by 1.7‰ compared to soft tissues is similar to the offset of +1.4‰
381 between bone collagen and hair obtained on modern individuals by O'Connell et al.
382 (2001).
- 383 - Rush fibres have the lowest $\delta^{13}\text{C}$ values (-24.4‰ and -24.6‰) of our collection of
384 samples.
- 385 - Concerning food remains, cereals are characterized by the lowest $\delta^{15}\text{N}$ values (4.0‰ and
386 5.2‰) while the fig has a $\delta^{15}\text{N}$ of 10.8‰. Animal leather and bone collagen have $\delta^{15}\text{N}$
387 values ranging from 6.5‰ to 11.2‰. Human bone collagens have the highest $\delta^{15}\text{N}$ values
388 ranging from 9.9‰ to 12.7‰. These data are compatible with a trophic chain that can be
389 reconstructed for Guayadeque and Acusa sites.
- 390 - Sixteen $\delta^{34}\text{S}$ values of human bone collagens are higher than 14.1‰ and up to 17.6‰
391 with an average value of 15.9 ± 0.9 ‰ that needs to be compared with the marine end-
392 member (present-day seawater has a $\delta^{34}\text{S}$ of 20.99 ± 0.25 ‰; Rees et al., 1978) that can be
393 estimated by the $\delta^{34}\text{S}$ of 20.3‰ measured in a *Patella* shell from the Bocabarranco site
394 (Gáldar) close to Agujero (Figure 1).
- 395 - Human bone collagen recovered from the sites occupied during the LIA have average
396 isotopic compositions which differ from those documented in sites occupied by humans
397 during the MWP by +0.5‰ for $\delta^{13}\text{C}$, +1.3‰ for $\delta^{15}\text{N}$ and +0.9‰ for $\delta^{34}\text{S}$ (Figure 5). In

398 addition, positive correlations are observed between $\delta^{15}\text{N}$ and $\delta^{13}\text{C}$ values ($R = 0.50$;
399 Figure 6) and between $\delta^{15}\text{N}$ and $\delta^{34}\text{S}$ values of human bone collagen ($R = 0.45$; Figure
400 7A). A more robust correlation ($R = 0.72$; Figure 7B) is obtained when excluding outlier
401 sample C4Ind10 from the Hormiguero site dated at 1000 to 1160 cal AD.

402

403 **5. Discussion**

404 *5.1. Update of the occupation chronology of the archaeological sites*

405 The new series of radiocarbon dating presented in this work, provides a new
406 framework to the recently proposed occupation processes of the island by the ancient
407 Canarians (Alberto et al. 2019; Velasco-Vázquez et al. 2019). In these processes, the inner
408 and mountain areas were the preferred landscapes by the first settlers arriving from the
409 northern areas of Africa around the 2nd–3rd centuries AD, while maintaining and increasing
410 the occupation of these areas over time. This scenario is exemplified by the new ^{14}C dates for
411 Guayadeque, Acusa and Andén del Tabacalete. In the case of Maspalomas and El Agujero-La
412 Guancha, the new dates reveal that the coastline started to be densely and extensively
413 populated by the ancient Canarians from the 13th century, but not as soon as the 11th century
414 as believed so far. Stone house villages with necropolises of pits and cists spread out along
415 the coast, especially on the fertile plains of ravine mouths.

416 This trend observed in the occupation of the island fits in with the most recent
417 proposals of social and economic changes over time, in the framework of intensification of
418 agricultural activity together with demographic growth (Alberto et al., 2019; Morales, 2019;
419 Moreno, 2014; Moreno Benítez and González Quintero, 2014; Velasco-Vázquez, 2014).

420 The new radiocarbon data also reinforce our knowledge of the diachrony of the
421 different funerary expressions, since sepulchral caves such as Acusa, Guayadeque or
422 Hormiguero were occupied at different times of the pre-Hispanic period, whereas cist and pit

423 necropolises such as Maspalomas or El Agujero-La Guancha developed during the 13th–14th
424 centuries.

425

426 *5.2. A record of climate change during the transition between the MWP and the LIA*

427 *5.2.1. Altitude effect on air temperatures and isotopic compositions of precipitations*

428 First of all, it must be kept in mind that the relationships between the present-day
429 environmental parameters of interest (LMWL, MAAT and isotopic altitudinal gradients) are
430 considered to be still valid when applied to the periods comprised between the 7th and 14th
431 centuries. It is probably a robust assumption to consider that these relationships are
432 conservative for at least the second half of the Holocene (e.g. Rozanski, 1985; Von
433 Grafenstein et al., 1996).

434 Hydrogen and oxygen isotope compositions of fresh waters collected in Gran Canaria
435 reflect, at the first order, the local meteoric water line of a tropical island as shown by the
436 properties of the linear regression equation ($S = 5.54$; $d = 5.42$; $R = 0.97$) illustrated in Figure
437 2. Consequently, changes in mean annual air temperatures are estimated by using the
438 following set of equations. Firstly, the relationship established between the $\delta^{18}\text{O}_{\text{mw}}$ and the
439 altitude in meters (m) (§section 4.2):

440

$$441 \delta^{18}\text{O}_{\text{mw}} (\text{‰}) = -0.00197(\pm 0.00091)\text{m} - 2.69(\pm 0.50) \quad (1)$$

442

443 is used to correct the $\delta^{18}\text{O}_{\text{p}}$ of pre-Hispanic individuals from the altitude effect upon
444 the isotopic composition of precipitation (Supplementary Table 3). Such corrections allow a
445 comparison of pre-Hispanic individuals within the same reference frame (cf. sea level).
446 Secondly, we took advantage of the relationship between altitude and mean annual air

447 temperature (Figure 8A), which has been established according to geographic and climatic
448 data published in Ninyerola et al. (2005), Martin (2006) and García de Diego et al. (2011):

449

$$450 \text{ MAAT} = -0.0044(\pm 0.0004)m + 21.49(\pm 0.44) \quad (2)$$

451

452 The Pearson's product moment correlation was performed to test the null hypothesis
453 H_0 of no correlation between the two studied variables; a p-value of 0.002 supports the
454 significance of this linear correlation. Moreover, the robustness of equation (2) is also
455 confirmed by its comparison, within the uncertainties, to that defined in Tenerife Island by
456 Yanes et al. (2009) who determined a relationship as follows:

457

$$458 \text{ MAAT} = -0.005m + 20.5 \quad (3)$$

459

460 Thirdly, by combining equations (1) and (2), we related MAAT to $\delta^{18}\text{O}_{\text{mw}}$ in Gran Canaria as
461 follows:

462

$$463 \text{ MAAT} = -0.0044(\pm 0.0004) \times \frac{(\delta^{18}\text{O}_{\text{mw}} + 2.69(\pm 0.50))}{-0.00197(\pm 0.00091)} + 21.49(\pm 0.44) \quad (4)$$

464

465 Equation (4) thus allowed us to calculate a difference in MAAT of $5 \pm 3^\circ\text{C}$
466 corresponding to the difference in the mean compositions of drinking water ($\Delta\delta^{18}\text{O}_p =$
467 2.3 ± 1.9) calculated between the LIA and MWP periods (Figure 4). The estimated uncertainty
468 of $\pm 3^\circ\text{C}$ associated with the change in MAAT is high because of the propagation of several
469 sources of uncertainties of which the most critical are the relationship between the $\delta^{18}\text{O}_p$ and
470 the $\delta^{18}\text{O}_{\text{mw}}$, and the $\delta^{18}\text{O}_{\text{mw}}$ and altitude. Indeed, in the case of equation (1), we emphasize
471 again that the location of water sampling may differ from the catchment area.

472 The present-day relationship between MAAT and $\delta^{18}\text{O}_{\text{mw}}$ in Tenerife (IAEA/WMO
473 data) indicates that a 2.3‰ change in seasonal variations of $\delta^{18}\text{O}_{\text{mw}}$ corresponds to a change
474 in $4.6(\pm 0.5)^\circ\text{C}$ in air temperature (Figure 8B). A result in accordance with that deduced from
475 the change in air temperature with altitude according to equation (2). Therefore, according to
476 equation (4), we consider that a drop in air temperature close to 4°C – 5°C (from about 22°C –
477 23°C down to 18°C – 17°C) is the most probable scenario that took place in Gran Canaria at
478 the beginning of the 14th century. The next step is to evaluate how this cooling event recorded
479 in Gran Canaria compares with the global picture of climate change during the MWP–LIA
480 transition.

481

482 *5.2.2. Climate change in Gran Canaria and the LIA cooling event*

483 As seen in section 4.3, assuming that the oxygen isotope composition of seawater did
484 not change in the eastern part of the Central Atlantic Ocean during the two last millennia,
485 since a seawater temperature of $22\pm 1^\circ\text{C}$ was inferred from the $\delta^{18}\text{O}_{\text{p}}$ of a parrotfish tooth.
486 Such temperature is in accordance with those ($20.7^\circ\text{C} < \text{mean } T < 22.4^\circ\text{C}$) calculated from
487 the oxygen isotope compositions of *Patella* shells coming from the western Canary Islands
488 (Tenerife, La Palma, La Gomera) and dated from 700 to 1200 AD (Parker et al., 2020). Sea
489 surface temperatures close to 21°C – 22°C recorded during the MWP resemble those
490 documented today off the Canary Archipelago with a mean SST of 20.4°C for the period
491 comprised between 2007 and 2017 (Meco et al., 2018). Similar observations have been made
492 from a stable isotope study of planktonic foraminifera (deMenocal et al., 2000) extracted from
493 Core 1H of ODP Hole 685C off Cap Blanc, Mauritania ($20^\circ 45' \text{N}$ – $18^\circ 35' \text{W}$). This
494 sedimentary record also revealed that SST were reduced in the tropical ocean by 3°C to 4°C
495 as soon as 1300 AD (deMenocal et al., 2000). These authors also attributed these SST

496 fluctuations to changes in the strength of the Canary Current, which is known to transport
497 temperate to subpolar waters throughout the European margin and West African coast.

498 The onset of colder climatic conditions during the LIA was recorded all along the
499 Atlantic rim including Greenland, Caribbean Islands, South America, South to Northwestern
500 Africa, and Western Europe (Supplementary Figure 1; Supplementary Table 1 and references
501 therein). Such observations led Lund et al. (2006) to consider a weakening of the North
502 Atlantic subtropical gyre accompanied by a southward motion of the Inter Tropical
503 Convergence Zone (ITCZ). A southward drift of about 5° in latitude of the ITCZ during the
504 LIA might be forced by a decrease in solar irradiance (Sachs et al., 2009). Paasche and Bakke
505 (2010) proposed on the basis of proxy observations that the atmosphere was the key “*of the*
506 *dynamical changes associated with the LIA and that major circulation patterns fluctuated on*
507 *century-time scales during interglacial climate conditions*”. Considering the cooling event,
508 which was contemporaneous with the beginning of the LIA, and affected the pre-Hispanic
509 populations of the Canary Islands, we can ask whether such a climatic perturbation
510 significantly impacted or not their diet, itself reflecting a potential major change in resource
511 availability.

512

513 *5.3. Did the climate change impact the diet of pre-Hispanic populations?*

514 Individuals dated from the 7th century (Guadayeque, Tejeda, Acusa) and individuals
515 dated from the 14th century (Maspalomas, Agujero) lived under different climatic conditions,
516 respectively the Medieval Warm Period (MWP) and the Little Ice Age (LIA). A difference in
517 $\delta^{18}\text{O}$ values of drinking water has been detected between these groups, representing
518 differences in mean air temperatures (Figure 4). In order to track the diet of pre-Hispanic
519 populations, we combined the analysis of three stable isotope systems ($\delta^{13}\text{C}$, $\delta^{34}\text{S}$ and $\delta^{15}\text{N}$) in
520 bone collagen and soft tissues of mummified human bodies.

521 The carbon isotope signal recorded in bone collagen is mainly influenced by diet in
522 vegetal species (C3/C4) and marine products (e.g. Schwarcz and Schoeninger, 1991). C3
523 species (wheat, barley) have been found in several archeological sites, showing that the
524 vegetal diet of pre-Hispanic populations was made up of C3 plants. Modern wheat and barley
525 have $\delta^{13}\text{C}$ values between -25.0‰ and -23.4‰ (Arnay-de-la-Rosa et al., 2010), fitting the
526 range of C3 plants. Carbon isotope values of archeological seeds, measured in the sites of
527 Guadayeque and Acusa, fall in the same isotopic range (Supplementary Table 4). While C3-
528 eaters have a carbon isotope value of $\approx -20\text{‰}$ (Richard and Hedges, 1999), there is a need to
529 assess the $\delta^{13}\text{C}$ signature of seafood eaters. Richard and Hedges (1999) estimated that
530 individuals with a 100% seafood diet should have $\delta^{13}\text{C}$ values similar to that of marine
531 mammals of approximately -12‰ . Considering two end-members for the diet (full C3 eater
532 and full seafood eater), we can estimate the proportions of vegetables and seafood in the diet
533 of individuals using a mass balance equation. For individuals that lived during the MWP, the
534 average $\delta^{13}\text{C}$ values of human bone collagen is $-19.6\pm 0.41\text{‰}$, while for those of the LIA the
535 average $\delta^{13}\text{C}$ value is $-19.08\pm 0.31\text{‰}$ (Supplementary Table 4; Figure 5). We thus obtained a
536 ratio between seed±cattle and seafood proportions of 95%–5% during the MWP and 89%–
537 11% during the LIA. Consequently, the diet of the LIA individuals seems to contain more
538 seafood products, by about 6% more than during the MWP, which is consistent with the
539 coastal positions of Maspalomas and Agujero.

540 Nitrogen isotopes are also powerful tracers of trophic chains as observed in Acusa and
541 Guayadeque (Figure 1). Indeed, an increase in $\delta^{15}\text{N}$ values from $+2.8$ to $+3.7\text{‰}$ is observed
542 throughout the trophic chain, which levels are cereals±fruits, cattle, and humans. This isotopic
543 fractionation of metabolic origin, which took place from one trophic level to the next, has a
544 magnitude comparable to those previously reported (from $+3$ to $+4\text{‰}$) in the literature (e.g.
545 Minagawa and Wada, 1984; Schoeninger and DeNiro, 1984; Kim et al., 2012).

546 The “LIA population” is also ^{15}N -enriched by $\approx 1.3\text{‰}$ compared to the MWP
547 population (Figure 5). On the basis of $\delta^{15}\text{N}$ values of human bone collagen, the proportion of
548 seafood consumption is estimated to be close to 20% by assuming a baseline of 9.9‰ (the
549 lowest observed value for sample 29.983, 7th, from Tejeda, inland; Figure 1; Supplementary
550 Table 4) for the $\delta^{15}\text{N}$ values of human bone collagen derived from a diet strictly based on the
551 consumption of terrestrial products, and a second end-member (mean $\delta^{15}\text{N} = 16.5\text{‰}$;
552 Schoeninger and DeNiro, 1984; Nehlich, 2015) based on a diet strictly composed of marine
553 fish and mammals. At variance with the previous estimate, nitrogen isotope ratios allow the
554 calculation of a proportion of marine products in the diet of humans about twice those
555 estimated from carbon isotope ratios. In the case of Gran Canaria there is a large number of
556 archaeological and anthropological evidence that points to the importance of fishing,
557 especially from the 12th–13th centuries AD (Rodríguez Santana, 1996; Velasco et al., 2000;
558 Delgado-Darias et al., 2005; 2006). The consumption levels of fish by the ancient Canarians,
559 at least at their final stage, are higher than those documented for the rest of the islands, where
560 seashells were the preferred marine products (Arnay-de-la Rosa et al., 2009; 2010). Fish is
561 ^{15}N -enriched as a consequence of longer trophic chains in marine ecosystems (Schoeninger
562 and DeNiro, 1984), which results in a higher $\delta^{15}\text{N}$ signature of human bone collagen than what
563 was expected from carbon isotope ratios. Therefore, we highlight that the nitrogen isotope
564 signature of the LIA population indicates an increased consumption of fish, among all
565 seafood products, as shellfish is less ^{15}N -enriched than fish as a consequence of shorter
566 trophic chains (Arnay-de-La-Rosa et al; 2010). When combining the carbon and nitrogen
567 isotope ratios (Figure 6), we observe the same increase in the marine component of the diet
568 when population migrated to the coast, as it has been shown in other studies conducted in
569 Southern California (Walker and DeNiro, 1986) or in British Columbia (Schwarcz et al.,
570 2014).

571 There is minute biological fractionation of sulfur ($0.5‰ \pm 2.4‰$) during food
572 assimilation (Nehlich, 2015), which implies that sulfur isotope ratios remain preserved
573 throughout the food chain (Krouse et al., 1991; Thode, 1991; McCutchan, et al., 2003). In
574 Gran Canaria, the sulfur isotope ratios of human bone collagen are always high
575 (Supplementary Table 4), thus reflecting a contamination of the whole trophic chain by the
576 well-known “sea spray effect” (Krouse et al., 1991; Thode, 1991; Thompson et al., 2010;
577 Nehlich, 2015). Diets based on terrestrial resources tend to have lower $\delta^{34}\text{S}$ values
578 (Thompson et al., 2010). The consumption of marine food is also responsible for high $\delta^{34}\text{S}$
579 values. In the case of Gran Canaria, an increase in consumption of marine products is
580 consistent with the higher average $\delta^{34}\text{S}$ value of the LIA population by $\approx 0.9‰$ compared to
581 that during the MWP (Figure 5). The location of the LIA population at Agujero and
582 Maspalomas, which are essentially on the coast, also explains that they were more likely to
583 consume seafood and fish compared to the MWP population which lived inland (Figure 1).
584 On the basis of $\delta^{34}\text{S}$ values, the proportion of seafood consumption is estimated to be close to
585 $13 \pm 10\%$ by assuming a baseline of $14‰$ (the lowest observed value is for sample 29.983, 7th
586 century AD, coming from Tejeda, inland; Figure 1; Supplementary Table 4) for the $\delta^{34}\text{S}$
587 values of human bone collagen only contaminated by sea spray and a marine end-member
588 value set to $21‰$, which is the ratio of modern seawater sulfate (Rees et al., 1978). Within the
589 large uncertainties associated with those calculations, we may consider that both estimates of
590 seafood proportion (a few wt%) in the diet are comparable on the basis of $\delta^{13}\text{C}$ and $\delta^{34}\text{S}$
591 proxies. Figure 7B also shows a combined increase in nitrogen and sulfur isotope ratios
592 between the “MWP” and the “LIA” populations, which is interpreted as a higher fish
593 consumption. This result supports the observations made from nitrogen and carbon isotope
594 ratios, pointing altogether toward a higher marine food consumption for the “LIA”
595 population. It is thus likely that the inhabitants migrated toward living areas close to the

596 coastline where less harsh climatic conditions prevailed than in altitude. Consequently, they
597 started to consume a significant amount of marine food relative to the diet of pre-Hispanic
598 people in Gran Canaria. However, these “LIA” populations conserved a diet mainly based on
599 the consumption of resources of terrestrial origin, thus revealing a form of cultural resilience
600 despite the colder and more arid conditions of the LIA compared to the MWP. These
601 conclusions concur with the results obtained by Arnay-de-La-Rosa et al (2009; 2010) and lead
602 to the same conclusion of a significant marine food consumption by the ancient Canarians in a
603 very advanced period of their historical development.

604

605 **6. Conclusion**

606 Radiocarbon dates of human collagen from the pre-Hispanic population of Gran
607 Canaria at six distinct archaeological localities revealed different periods of human
608 occupation between the beginning of the 7th and the mid-14th century. The dates obtained
609 cover the transition between the Medieval Warm Period (MWP) and the onset of the Little Ice
610 Age (LIA).

611 Over this time interval, the oxygen isotope compositions of apatite phosphate ($\delta^{18}\text{O}_p$)
612 from bones of pre-Hispanic individuals revealed a decrease from -2.1‰ to -4.4‰ of meteoric
613 waters, which is interpreted as a decrease in air temperature by about $5\pm 3^\circ\text{C}$. Our result is
614 consistent with the sedimentary isotopic record in Core 1H of ODP Hole 685C off Cap Blanc,
615 Mauritania where SST started to decrease by 3°C to 4°C at the beginning of the 14th century.
616 Such cooling event most likely resulted from a major reorganization of atmospheric and
617 oceanic circulations in the North Atlantic Ocean forced by a decrease in solar irradiance.

618 The stable isotope compositions (C, N and S) of soft tissues suggest that the pre-
619 Hispanic population from Gran Canaria relied mostly on agriculture and the contribution of
620 seafood products, especially fishes, to their diet was identified in archaeological sites of

621 Agujero and Maspalomas located near the coast, with occupation dated contemporaneous to
622 the LIA.

623 Our results inferred from stable isotope data and ¹⁴C dating of human remains suggest
624 that the pre-Hispanic population of Gran Canaria developed a resilience to climate change,
625 reflected in a relatively steady composition of diet over a time interval between the beginning
626 of the 7th century and the first half of the 14th century.

627

628 **Acknowledgements** – The authors are grateful to the technical and administrative staff (M.C.
629 Cruz de Mercadal and A. Betancor Rodríguez) of El Museo Canario, Gran Canaria, for their
630 warm welcome, and thorough preparation, referencing and packaging of archeological
631 samples. U. Brand is thanked for editing this manuscript. This study was funded by the Centre
632 National de la Recherche Scientifique and the Institut Universitaire de France (CL).

633

634

635 **References**

636

637 Alberto, V., Delgado, T., Moreno, M. A., Velasco, J., (2019) La dimensión temporal y el
638 fenómeno sepulcral entre los antiguos canarios. *Zephyrus* 84, 139–160.

639 Alberto, V., and Velasco Vázquez, J., 2009-2010. Manipulación del cadáver y práctica
640 funeraria entre los antiguos canarios: la perspectiva osteoarqueológica. *Tabona. Revista de*
641 *Prehistoria y de Arqueología* 18, 91–120.

642 Alberto, V., Delgado, T., Velasco, J., Santana, J., 2014. En la ambigüedad de tu piel. Sobre
643 momias y tumbas. *Revista de Prehistoria y de Arqueología* 20, 33–60.

644 Alberto, V., Moreno, M., Alamón, M., Suárez, I., Mendoza, F., 2017. Estudio
645 zooarqueológico de la Restinga (Gran Canaria, España). Datos para la definición de un
646 modelo productivo. *XXII Coloquio de Historia Canario-Americana* (2016), XXII-137.
647 <http://coloquioscanariasamerica.casadecolon.com/index.php/aea/article/view/10074>

648 Arnaiz-Villena, A., Muñiz, E., Campos, C., Gomez-Casado, E., Tomasi, S., Martínez-Quiles,
649 N., Martín-Villa, M., Palacio-Gruber, J., 2015. Origin of Ancient Canary Islanders
650 Guanches: presence of Atlantic/Iberian HLA and Y chromosome genes and Ancient
651 Iberian language. *International Journal of Modern Anthropology* 1, 67–93.

652 Arnay-de-la-Rosa, M., Gámez-Mendoza, A., Navarro-Mederos, J. F., Hernández-Marrero, J.
653 C., Fregel, R., Yanes, Y., Galindo-Martín, L., Romanek, C.S. González-Reimers, E., 2009.
654 Dietary patterns during the early prehispanic settlement in La Gomera (Canary
655 Islands). *Journal of Archaeological Science* 36, 1972–1981.

656 Arnay-de-la-Rosa, M., González-Reimers, E., Yanes, Y., Velasco-Vázquez, J., Romanek
657 C.S., Noakes, J.E., 2010. Paleodietary analysis of the prehistoric population of the Canary
658 Islands inferred from stable isotopes (carbon, nitrogen and hydrogen) in bone collagen.
659 *Journal of Archaeological Science* 37, 1490–1501.

660 Arneborg, J., Heinemeier, J., Lynnerup, N., Nielsen, H. L., Rud, N., & Sveinbjörnsdóttir, Á.
661 E., 2002. C-14 dating and the disappearance of Norsemen from Greenland. *Europhysics*
662 *News* 33, 77–80.

663 Athimon, E., and Maanan, M., 2018. Vulnerability, resilience and adaptation of societies
664 during major extreme storms during the Little Ice Age. *Climate of the Past* 14, 1487–1497.

665 Brönnimann, S., Franke, J., Nussbaumer, S. U., Zumbühl, H. J., Steiner, D., Trachsel, M.,
666 Hegerl, G. C., Schurer, A., Worni, M., Malik, A., Flückiger, J., Raible, C. C., 2019. Last
667 phase of the Little Ice Age forced by volcanic eruptions. *Nature Geoscience* 12, 650–656.

668 Brown, E. T., and Johnson, T. C., 2005. Coherence between tropical East African and South
669 American records of the Little Ice Age. *Geochemistry, Geophysics, Geosystems* 6, 12.
670 doi:10.1029/2005GC000959

671 Büntgen, U., Myglan, V. S., Ljungqvist, F. C., McCormick, M., Di Cosmo, N., Sigl, M.,
672 Jungclaus, J., Wagner, S., Krusic, P. J., and Esper, J., 2016. Cooling and societal change
673 during the Late Antique Little Ice Age from 536 to around 660 AD. *Nature Geoscience* 9,
674 231–236.

675 Büntgen, U., Tegel, W., Nicolussi, K., McCormick, M., Frank, D., Trouet, V., Kaplan, J. O.,
676 Herzig, F., Heussner, K.-U., Wanner, H., Luterbacher, J., and Esper, J., 2011. 2500 years
677 of European climate variability and human susceptibility. *Science* 331, 578–582.

678 Clauzel, T., Maréchal, C., Fourel, F., Barral, A., Amiot, R., Betancort, J. F., Lomoschitz, A.,
679 Meco, J., Lécuyer, C., 2020. Reconstruction of sea-surface temperatures in the Canary
680 Islands during Marine Isotope Stage 11. *Quaternary Research* 94, 195–209.

681 D’Andrea, W. J., Huang, Y., Fritz, S. C., Anderson, N. J., 2011. Abrupt Holocene climate
682 change as an important factor for human migration in West Greenland. *Proceedings of the*
683 *National Academy of Sciences* 108, 9765–9769.

684 Dansgaard, W., 1964. Stable isotopes in precipitation. *Tellus* 16, 436–468.

685 Daux, V., Lécuyer, C., Héran, M. A., Amiot, R., Simon, L., Fourel, F., Martineau, F.,
686 Lynnerup, N., Reyhler, H., Escarguel, G., 2008. Oxygen isotope fractionation between
687 human phosphate and water revisited. *Journal of Human Evolution* 55, 1138–1147.

688 Delgado-Darias, T., 2009. *La historia en los dientes: una aproximación a la prehistoria de*
689 *Gran Canaria desde la antropología dental*. Las Palmas de Gran Canaria: Ediciones
690 Cabildo de Gran Canaria.

691 Delgado-Darias, T., 2020. La medida del tiempo. El Museo Canario Pieza del mes. Retrieved
692 from
693 [http://www.elmuseocanario.com/images/documentospdf/piezadelmes/2020/piezafebrero20](http://www.elmuseocanario.com/images/documentospdf/piezadelmes/2020/piezafebrero2020.pdf)
694 [20.pdf](http://www.elmuseocanario.com/images/documentospdf/piezadelmes/2020/piezafebrero2020.pdf).

695 Delgado-Darias, T., Velasco-Vázquez, J., Arnay-De-La-Rosa, M., Martín-Rodríguez, E.,
696 González-Reimers, E., 2006. Calculus, periodontal disease and tooth decay among the
697 prehispanic population from Gran Canaria. *Journal of Archaeological Science* 33, 663–
698 670.

699 Delgado-Darias, T., Velasco-Vázquez, J., Arnay-de-la-Rosa, M., Martín-Rodríguez, E.,
700 González-Reimers, E., 2005. Dental caries among the prehispanic population from Gran
701 Canaria. *American Journal of Physical Anthropology* 128, 560–568.

702 DeMenocal, P. B., 2001. Cultural responses to climate change during the late
703 Holocene. *Science* 292, 667–673.

704 DeMenocal, P. B., Ortiz, J., Guilderson, T., Sarnthein, M., 2000. Coherent high-and low-
705 latitude climate variability during the Holocene warm period. *Science* 288, 2198–2202.

706 DeNiro, M. J., 1985. Postmortem preservation and alteration of in vivo bone collagen isotope
707 ratios in relation to palaeodietary reconstruction. *Nature* 317, 806–809.

708 Dugmore, A., J., Keller, C., McGovern, T., H., 2007. Norse Greenland Settlement:
709 Reflections on Climate Change, Trade, and The Contrasting Fates of Human Settlements
710 in the North Atlantic Islands. *Arctic Anthropology* 44, 12–36.

711 Easterbrook, D. J., 2016. Cause of Global Climate Changes: Correlation of Global
712 Temperature, Sunspots, Solar Irradiance, Cosmic Rays, and Radiocarbon and Beryllium
713 Production Rates. In: *Evidence-Based Climate Science*, Elsevier, 245–262 pp.

714 Fang, K., Chen, D., Ilvonen, L., Pasanen, L., Holmström, L., Seppä, H., Huang, G., Ou, T.,
715 Linderholm, H., 2019. Oceanic and atmospheric modes in the Pacific and Atlantic Oceans
716 since the Little Ice Age (LIA): Towards a synthesis. *Quaternary Science Reviews* 215,
717 293–307.

718 Fregel, R., Martínez V., Larruga, J. M., Hernández, J. C., Gámez, A., Pestano, J., Arnay, M.,
719 González, A. M., 2015. Isolation and prominent aboriginal maternal legacy in the present
720 day population of La Gomera (Canary Islands). *European Journal of Human Genetics* 23,
721 1236–1243.

722 Fregel, R., Gomes, V., Gusmao, L., González, A. N., Cabrera, V. M., Amorim, A., Larruga, J.
723 M., 2009. Demographic history of Canary Islands male gene-pool: replacement of native
724 lineages by European. *BMC Evolutionary Biology* 9, 181. doi:10.1186/1471-2148-9-181.

725 Fregel, R., Ordóñez, A. C., Santana, J., Cabrera, V. M., Velasco, J., Alberto, V., Moreno M.
726 A., Delgado, T., Rodríguez, A., Hernández, J. C., Pais, J., González, R., Lorenzo, J. M.,
727 Flores, C., Cruz, M. C., Álvarez, N., Shapiro, B., Arnay, M., Bustamante C. D., 2019.
728 Mitogenomes illuminate the origin and migration patterns of the indigenous people of the
729 Canary Islands. *PloS one*, 14(3). <https://doi.org/10.1371/journal.pone.0209125>

730 García de Diego, Margarita de Luxan, Reymundo Izard Araceli, 2011. *Manual de Diseño*
731 *Bioclimático para Canarias*. Las Palmas de Gran Canaria: ITC. Glimcher, M. J., 2006.
732 *Bone: Nature of the Calcium Phosphate Crystals and Cellular, Structural, and Physical*

733 Chemical Mechanisms in Their Formation. *Reviews in Mineralogy and Geochemistry* 64,
734 223–282.

735 Gonfiantini, R., Roche, M. A., Olivry, J. C., Fontes, J. C., Zuppi, G. M., 2001. The altitude
736 effect on the isotopic composition of tropical rains. *Chemical Geology* 181, 147–167.

737 González-Reimers, E., Velasco-Vázquez, J., Arnay-de-la-Rosa, M., Santolaria-Fernández, F.,
738 Gómez-Rodríguez, M. A., Machado-Calvo, M. 2002. Double-Energy X-Ray
739 Absorptiometry in the Diagnosis of Osteopenia in Ancient Skeletal Remains. *American*
740 *Journal of Physical Anthropology* 118, 134–145.

741 Guatelli-Steinberg, D., Irish, J., Lukacs, J., 2001. Canary Islands - North African population
742 affinities: measures of divergence based on dental morphology. *HOMO – Journal of*
743 *Comparative Human Biology* 52, 173–188.

744 Hagenblad, J., Morales, J., Leino, M. W., Rodríguez-Rodríguez, A.C., 2017. Farmer fidelity
745 in the Canary Islands revealed by ancient DNA from prehistoric seeds. *Journal of*
746 *Archaeological Science* 78, 78–87.

747 Henke, L. M., Lambert, F. H., Charman, D. J., 2017. Was the Little Ice Age more or less El
748 Niño-like than the Medieval Climate Anomaly? Evidence from hydrological and
749 temperature proxy data. European Geosciences Union (EGU) / Copernicus Publications.

750 Henríquez-Valido, P., Morales, J., Vidal-Matutano, P., Santana-Cabrera, J., Rodríguez
751 Rodríguez, A., 2019. Arqueoentomología y arqueobotánica de los espacios de
752 almacenamiento a largo plazo: el granero de Risco Pintado, Temisas (Gran Canaria).
753 *Trabajos de Prehistoria* 76, 120–137.

754 Holmgren, K., Tyson, P. D., Moberg, A., Svanered, O., 2001. A preliminary 3000-year
755 regional temperature reconstruction for South Africa. *South African Journal of Science* 97,
756 49–51.

757 Huffman, T. N., 1996. Archaeological evidence for climatic change during the last 2000 years
758 in southern Africa. *Quaternary International* 33, 55–60.

759 Ilyashuk, E. A., Heiri, O., Ilyashuk, B. P., Koinig, K. A., Psenner, R., 2019. The Little Ice
760 Age signature in a 700-year high-resolution chironomid record of summer temperatures in
761 the Central Eastern Alps. *Climate Dynamics* 52, 6953–6967.

762 Johnson, T. C., Barry, S. L., Chan, Y., Wilkinson, P., 2001). Decadal record of climate
763 variability spanning the past 700 yr in the Southern Tropics of East Africa. *Geology* 29,
764 83–86.

765 Kim, S. L., Casper, D. R., Galván-Magaña, F., Ochoa-Díaz, R., Hernández-Aguilar, S. B.,
766 Koch, P. L., 2012. Carbon and nitrogen discrimination factors for elasmobranch soft

767 tissues based on a long-term controlled feeding study. *Environmental Biology of*
768 *Fishes* 95, 37–52.

769 Koch, A., Brierley, C., Maslin, M. M., Lewis, S. L., 2019. Earth system impacts of the
770 European arrival and Great Dying in the Americas after 1492. *Quaternary Science*
771 *Reviews* 207, 13–36.

772 Kottek, M., Grieser, J., Beck, C., Rudolf, B., Rubel, F., 2006. World map of the Köppen-
773 Geiger climate classification updated. *Meteorologische Zeitschrift* 15, 259–263.

774 Krouse, H. R., Stewart, J. W. B., Grinenko, V. A., 1991. Pedosphere and biosphere. In:
775 Krouse, H. R., and Grinenko, V. A., editors. *Stable isotopes in the assessment of natural*
776 *and anthropogenic sulphur in the environment*. Chichester, Wiley, 267–304 pp.

777 Lamb, H. H., 1980. Climatic fluctuations in historical times and their connections with
778 transgressions of the sea, storm floods and other coastal changes, in: *Transgressies and*
779 *Occupatiegeschiedenis de kustgebieden van Nederland en België*, edited by Verhulst, A.
780 and Gottschalk, M. K. E., Belgisch Centron Voor Landelifke Greschiedenis, Gand, 251–
781 281 pp.

782 Lane, C., S., Horn, S., P., Orvis, K., H., Thomason, J., M., 2011. Oxygen isotope evidence of
783 Little Ice Age aridity on the Caribbean slope of the Cordillera Central, Dominican
784 Republic. *Quaternary Research* 75, 461–470.

785 Le Roy Ladurie, E., 1967. *L’histoire du climat depuis l’an mil*, Flammarion, Paris, 379 pp.

786 Le Roy Ladurie, E., 1971. *Times of Feast, Times of Famine*. Farrar, Strauss, and Giroux, New
787 York, 438 pp.

788 Lécuyer, C., Amiot, R., Touzeau, A., Trotter, J., 2013. Calibration of the phosphate $\delta^{18}\text{O}$
789 thermometer with carbonate–water oxygen isotope fractionation equations. *Chemical*
790 *Geology* 347, 217–226.

791 Lund, D. C., Lynch-Stieglitz, J., Curry, W. B., 2006. Gulf Stream density structure and
792 transport during the past millennium. *Nature* 444, 601–604.

793 Maca-Meyer, N., Arnay, M., Rando, J. C., Flores, C., González, A. M., Cabrera, V. M.,
794 Larruga, J. M., 2004. Ancient mtDNA analysis and the origin of the Guanches. *European*
795 *Journal of Human Genetics* 12, 155–162.

796 Macfarling Meure, C., Etheridge, D., Trudinger, C., Steele, P., Langenfelds, R., Van Ommen,
797 T., Smith, T. Elkins, J., 2006. Law Dome CO₂, CH₄ and N₂O ice core records extended to
798 2000 years BP. *Geophysical Research Letters*, 33, L14810, doi:10.1029/2006GL026152.

799 Mann, M. E., Zhang, Z., Rutherford, S., Bradley, R. S., Hughes, M. K., Shindell, D.,
800 Ammann, C., Faluvegi, C., Ni, F., 2009. Global signatures and dynamical origins of the
801 Little Ice Age and Medieval Climate Anomaly. *Science* 326, 1256–1260.

802 Marsicek, J., Shuman, B. N., Bartlein, P. J., Shafer, S. L., Brewer, S., 2018). Reconciling
803 divergent trends and millennial variations in Holocene temperatures. *Nature* 554, 92–96.

804 Martín, M., 2006. Calidad ambiental en la edificación para Las Palmas de Gran Canaria.
805 Manuales ICARO. Departamento de Construcción Arquitectónica Universidad de Las
806 Palmas de Gran Canaria.

807 Maslin, M., Stickley, C., Ettwein, V., 2001. Holocene climate variability. 1st edition of
808 *Encyclopedia of Ocean Sciences*, vol. 2, pp 1210–1217.

809 McCutchan Jr, J. H., Lewis Jr, W. M., Kendall, C., McGrath, C. C., 2003. Variation in trophic
810 shift for stable isotope ratios of carbon, nitrogen, and sulfur. *Oikos* 102, 378–390.

811 Meco, J., Lomoschitz, A., Rodriguez, A., Ramos, A. J. G., Betancort, J. F., Coca, J., 2018.
812 Mid and late Holocene sea level variations in the Canary Islands. *Palaeogeography*
813 *Palaeoclimatology Palaeoecology* 507, 214–225.

814 Miller, G. H., Geirsdóttir, Á., Zhong, Y., Larsen, D. J., Otto-Bliesner, Bette. L., Holland, M.
815 M., Bailey, D. A., Refsnider, K. A., Lehman, S. J., Southon, J. R., Anderson, C.,
816 Björnsson, H., Thordarson, T., 2012. Abrupt onset of the Little Ice Age triggered by
817 volcanism and sustained by sea-ice/ocean feedbacks. *Geophysical Research Letters* 39,
818 L02708, doi:10.1029/2011GL050168.

819 Minagawa, M., and Wada, E., 1984. Stepwise enrichment of ^{15}N along food chains: further
820 evidence and the relation between $\delta^{15}\text{N}$ and animal age. *Geochimica et Cosmochimica*
821 *acta* 48, 1135–1140.

822 Moberg, A., Sonechkin, D. M., Holmgren, K., Datsenko, N. M., Karlén, W., 2005. Highly
823 variable Northern Hemisphere temperatures reconstructed from low- and high-resolution
824 proxy data. *Nature* 433, 613–617.

825 Morales, J., 2019. Los guardianes de las semillas. Origen y evolución de la agricultura en
826 Gran Canaria. Colección La Isla de los Canarios, 2. Las Palmas de Gran Canaria: Ed.
827 Cabildo Insular Gran Canaria.

828 Morales, J., Rodríguez, A., González, M.C., Martín, E., Henríquez, P., Del Pino, M., 2014.
829 The archaeobotany of long-term crop storage in northwest African communal granaries: a
830 case study from pre-Hispanic Gran Canaria (cal. ad 1000-1500). *Vegetation History and*
831 *Archaeobotany* 23, 789–804.

832 Moreno Benítez, M. A., and González Quintero, P., 2014. Una perspectiva territorial al uso
833 del suelo en la Gran canaria prehispanica (siglos XI-XV). *Revista de Prehistoria y de*
834 *Arqueología* 20, 9–32.

835 Moreno, M.A., 2014. Desde arriba se ve mejor. Aproximación al uso del suelo en la Gran
836 Canaria prehispanica (ss. XI-XV). In Acosta Guerrero, E. (coord.) *XX Coloquio de*
837 *Historia Canario Americano*, pp. 1240–1256. Las Palmas de Gran Canaria: Cabildo de
838 Gran Canaria.

839 National Center for Atmospheric Research Staff. The Climate Data Guide: Global surface
840 temperatures. BEST: Berkeley Earth Surface Temperatures. Retrieved from [https://](https://climatedataguide.ucar.edu/climate-data/global-surface-temperatures-best-berkeley-earth-surface-temperatures)
841 [climatedataguide.ucar.edu/climate-data/global-surface-temperatures-best-berkeley-earth-](https://climatedataguide.ucar.edu/climate-data/global-surface-temperatures-best-berkeley-earth-surface-temperatures)
842 [surface-temperatures](https://climatedataguide.ucar.edu/climate-data/global-surface-temperatures-best-berkeley-earth-surface-temperatures).

843 Navarro Mederos, J.F., 1979. Excavaciones arqueológicas en «El Hormiguero de
844 Casablanca», Firgas (Gran Canaria). In *XV Congreso Nacional de Arqueología*, Zaragoza,
845 pp. 329-336.

846 Nehlich, O., 2015. The application of sulphur isotope analyses in archaeological research: a
847 review. *Earth-Science Reviews* 142, 1–17.

848 Ninyerola, M., Pons, X., Roure, J. M., 2005. *Atlas climático digital de la Península Ibérica*.
849 Universitat Autònoma de Barcelona.

850 O’Connell, T. C., and Hedges, R. E., 1999. Isotopic comparison of hair and bone:
851 archaeological analyses. *Journal of Archaeological Science* 26, 661–665.

852 O’Connell, T. C., Hedges, R. E., Healey, M. A., Simpson, A. H. R. W., 2001. Isotopic
853 comparison of hair, nail and bone: modern analyses. *Journal of Archaeological Science* 28,
854 1247–1255.

855 Ordoñez, A. C., Fregel, R., Trujillo-Mederos A., Hervella, M., De la Rúa, C., Arnay-de-la-
856 Rosa, M., 2017. Genetic studies on the prehispanic population buried in Punta Azul cave
857 (El Hierro, Canary Islands). *Journal of Archaeological Science* 78, 20–28.

858 Owens, M. J., Lockwood, M., Hawkins, E., Usoskin, I., Jones, G. S., Barnard, L., Schurer, A.,
859 Fasullo, J., 2017. The Maunder minimum and the Little Ice Age: an update from recent
860 reconstructions and climate simulations. *Journal of Space Weather and Space Climate* 7,
861 A33. doi.org/10.1051/swsc/2017034.

862 Paasche, Ø., Bakke, J., 2010. Defining the Little Ice Age. *Climate of the Past Discussions* 6,
863 2159–2175.

864 Parker, W., Yanes, Y., Mesa Hernández, E., Hernández Marrero, J. C., Pais, J., Soto
865 Contreras, N., Surge, D., 2020. Shellfish exploitation in the western Canary Islands over
866 the last two millennia. *Environmental Archaeology* 25, 14–36.

867 Pinto, F., González, A. M., Hernández, M., Larruga, J. M., & Cabrera, V. M., 1996. Genetic
868 relationship between the Canary Islanders and their African and Spanish ancestors inferred
869 from mitochondrial DNA sequences. *Annals of Human Genetics* 60, 321–330.

870 Prentice, R., 2009. Cultural responses to climate change in the Holocene. *Anthós* 1, 3. DOI:
871 10.15760/anthos.2009.41

872 Rando, J. C., Cabrera, V. M., Larruga, J. M., Hernández, M., González, A. M., Pinto, F.,
873 Bandelt, H. J., 1999. Phylogeographic patterns of mtDNA reflecting the colonization of the
874 Canary Islands. *Annals of Human Genetics* 63, 413–428.

875 Rees, C. E., Jenkins, W. J., Monster, J., 1978. The sulphur isotopic composition of ocean
876 water sulphate. *Geochimica et Cosmochimica Acta* 42, 377–381.

877 Richards, M. P., Hedges, R. E. M., 1999. Stable Isotope Evidence for Similarities in the
878 Types of Marine Foods Used by Late Mesolithic Humans at Sites Along the Atlantic Coast
879 of Europe. *Journal of Archaeological Science* 26, 717–722.

880 Robertson, A., Overpeck, J., Rind, D., Mosley-Thompson, E., Zielinski, G., Lean, J., Koch,
881 D., Penner, J., Tegen, I., Healy, R., 2001. Hypothesized climate forcing time series for the
882 last 500 years. *Journal of Geophysical Research: Atmospheres*, 106, 14783–14803.

883 Rodríguez Santana, C. G., 1996. La pesca entre los Canarios, Guanches y Auaritas. Las
884 Palmas de G.C. Ed. Cabildo Insular de Gran Canaria.

885 Rodríguez-Varela, R., Günther, T., Krzewińska, M., Storå, J., Gillingwater, T. H.,
886 MacCallum, M., Arsuaga, J. L., Dobney, K., Valdiosera, C., Jakobsson, M., Götherström,
887 A., Girdland-Flink, L., 2017. Genomic analyses of Pre-European conquest human remains
888 from the Canary Islands reveal close affinity to modern North Africans. *Current*
889 *Biology* 27, 3396–3402.

890 Rozanski, K., 1985. Deuterium and Oxygen-18 in European groundwaters—links to
891 atmospheric circulation in the past. *Chemical Geology* 52, 349–363.

892 Russell, J. M., Verschuren, D., Eggermont, H., 2007. Spatial complexity of ‘Little Ice Age’
893 climate in East Africa: sedimentary records from two crater lake basins in western
894 Uganda. *The Holocene* 17, 183–193.

895 Sachs, J. P., Sachse, D., Smittenberg, R. H., Zhang, Z. H., Battisti, D. S., Golubic, S., 2009.
896 Southward movement of the Pacific intertropical convergence zone AD 1400–1850,
897 *Nature Geoscience* 2, 519–525.

- 898 Santana Cabrera, J., Velasco Vázquez, J., Rodríguez Rodríguez, A. C., 2012. Patrón cotidiano
899 de actividad física y organización social del trabajo en la Gran Canaria prehistórica (siglos
900 XI-XV): la aportación de los marcadores óseos de actividad física. *Revista de Prehistoria y*
901 *Arqueología* 19, 125–163.
- 902 Santos, C., Fregel, R., Cabrera, V. M., González, A. M., Larruga, J. M., Lima, M., 2010.
903 Mitochondrial DNA patterns in the Macaronesia islands: variation within and among
904 archipelagos. *American Journal of Physical Anthropology* 141, 610–619.
- 905 Schoeninger, M. J., and DeNiro, M. J., 1984. Nitrogen and carbon isotopic composition of
906 bone collagen from marine and terrestrial animals. *Geochimica et Cosmochimica Acta* 48,
907 625–639.
- 908 Schwarcz, H. P., Chisholm, B. S., Burchell, M., 2014. Isotopic studies of the diet of the
909 people of the coast of British Columbia. *American Journal of Physical Anthropology* 155,
910 460–468.
- 911 Schwarcz, H. P., and Schoeninger, M. J., 1991. Stable isotope analyses in human nutritional
912 ecology. *American Journal of Physical Anthropology* 34, 283–321.
- 913 Shindell, D. T., Schmidt, G. A., Miller, R. L., Mann, M. E., 2003. Volcanic and solar forcing
914 of climate change during the preindustrial era. *Journal of Climate* 16, 4094–4107.
- 915 Siegenthaler, U. R. S., Monnin, E., Kawamura, K., Spahni, R., Schwander, J., Stauffer, B.,
916 Stocker, T.F., Barnola, J.-M., Fischer, H., 2005. Supporting evidence from the EPICA
917 Dronning Maud Land ice core for atmospheric CO₂ changes during the past
918 millennium. *Tellus B: Chemical and Physical Meteorology* 57, 51–57.
- 919 Soon, W., and Baliunas, S., 2003. Proxy climatic and environmental changes of the past 1000
920 years. *Climate Research* 23, 89–110.
- 921 Thode, H. G., 1991. Sulphur isotopes in nature and the environment: an overview. In: Krouse,
922 H. R., and Grinenko, V.A. (eds.). *Stable Isotopes: Natural and Anthropogenic Sulphur in*
923 *the Environment*. John Wiley & Sons, Chichester, 43, 1–26.
- 924 Thompson, A. H., Chesson, L. A., Podlesak, D. W., Bowen, G. J., Cerling, T. E., Ehleringer,
925 J. R., 2010. Stable isotope analysis of modern human hair collected from Asia (China,
926 India, Mongolia, and Pakistan). *American Journal of Physical Anthropology* 141, 440–451.
- 927 Thordarson, T., and Self, S., 1993. The Laki (Skaftár Fires) and Grímsvötn eruptions in 1783–
928 1785. *Bulletin of Volcanology* 55, 233–263.
- 929 Touzeau, A., Blichert-Toft, J., Amiot, R., Fourel, F., Martineau, F., Cockitt, J., Hall, K.,
930 Flandrois J.-P., Lécuyer, C., 2013. Egyptian mummies record increasing aridity in the Nile

931 valley from 5500 to 1500 yr before present. *Earth and Planetary Science Letters* 375, 92–
932 100.

933 Tyson, P. D., Karlen, W., Holmgren, K., Heiss, G. A., 2000. The Little Ice Age and medieval
934 warming in South. *South African Journal of Science* 96, 121–126.

935 Van Klinken, G.J., 1999. Bone collagen quality indicators for palaeodietary and radiocarbon
936 measurements. *Journal of Archaeological Science* 26, 687–695.

937 Velasco-Vázquez, J., 2014. El tiempo de los antiguos canarios. *Boletín electrónico de*
938 *Patrimonio Histórico* 2, 12–15.

939 Velasco-Vázquez, J., Alberto-Barroso, V., Delgado-Darias, T., Moreno-Benítez, M., Lécuyer,
940 C., Richardin, P., 2019. Poblamiento, colonización y primera historia de Canarias: el C14
941 como paradigma. *Anuario de Estudios Atlánticos* 66, 066-001.

942 Velasco-Vázquez, J., Betancor-Rodríguez, A., Arnay-De-La Rosa, M., Gonzalez-Reimers, E.,
943 2000. Auricular exostoses in the prehistoric population of Gran Canaria. *American Journal*
944 *of Physical Anthropology* 112, 49–55.

945 Verschuren, D., Laird, K. R., Cumming, B. F., 2000. Rainfall and drought in equatorial east
946 Africa during the past 1,100 years. *Nature* 403, 410–414.

947 Vidal-Matutano, P. Morales, J., Henríquez-Valido, P., Marchante Ortega, A., Moreno
948 Benítez, M., Rodríguez-Rodríguez, A., 2020. El uso de la madera en espacios de
949 almacenamiento colectivos: análisis xilológico y antracológico de los silos prehispánicos
950 (ca.500 – 1500 D.C.) de La Fortaleza (Santa Lucía de Tirajana, Gran Canaria). *Vegueta* 20,
951 469–489.

952 Von Grafenstein, U., Erlenkeuser, H., Müller, J., Trimborn, P., Alefs, J., 1996. A 200 year
953 mid-European air temperature record preserved in lake sediments: An extension of the
954 $\delta^{18}\text{O}_p$ -air temperature relation into the past. *Geochimica et Cosmochimica Acta* 60, 4025–
955 4036.

956 Walker, P. L., and DeNiro, M. J., 1986. Stable nitrogen and carbon isotope ratios in bone
957 collagen as indices of prehistoric dietary dependence on marine and terrestrial resources in
958 southern California. *American Journal of Physical Anthropology* 71, 51–61.

959 Yanes, Y., Romanek, C. S., Delgado, A., Brant, H. A., Noakes, J. E., Alonso, M. R., Ibáñez,
960 M., 2009. Oxygen and carbon stable isotopes of modern land snail shells as environmental
961 indicators from a low-latitude oceanic island. *Geochimica et Cosmochimica Acta* 73 4077–
962 4099.

963 Zharkova, V. V., Shepherd, S. J., Zharkov, S. I., Popova, E., 2019. Oscillations of the baseline
964 of solar magnetic field and solar irradiance on a millennial timescale. *Scientific Reports* 9,
965 1–12.
966
967
968

969

970 **Figure captions:**

971

972 Figure 1: Geographic maps of the Canary Archipelago and of the island of Gran Canaria with
973 the location of studied archaeological sites (filled red circles) and sampled marine and
974 fresh waters (filled blue circles). Pictures were taken from Google EarthTM. Numbers
975 in brackets represent the range and standard deviation around the mean of $\delta^{18}\text{O}_p$ values
976 of Canarian skeletal remains.

977

978 Figure 2: A) $\delta^2\text{H}-\delta^{18}\text{O}$ (‰ VSMOW) bivariate plot for Gran Canaria marine waters (filled
979 blue circles), fresh waters (filled green circles), SMOW (filled red square). The black
980 line illustrates the Global Meteoric Water Line (GMWL). B) Linear fit of fresh water
981 $\delta^2\text{H}-\delta^{18}\text{O}$ data defines a slope S of 5.54 ± 0.52 and an intercept d of 5.42 ± 1.95 ($R =$
982 0.97 ; $n = 10$); both being characteristics of Local Meteoric Water Lines observed in
983 tropical islands.

984

985 Figure 3: $\delta^{18}\text{O}_{\text{mw}}$ -altitude bivariate plot for Gran Canaria fresh water samples. Altitude is
986 reported in meters above sea level (m a.s.l.). A linear fit of data defines a slope of -
987 0.00197 ± 0.00091 and an intercept of -2.69 ± 0.50 ($R = -0.61$; $n = 10$). Sample GC-6 has
988 been discarded from the data set (Supplementary Table 5) as $\delta^2\text{H}$ and $\delta^{18}\text{O}$ values
989 close to the SMOW composition suggest a significant rate of evaporation while water
990 was resting in the pond.

991

992 Figure 4: Oxygen isotope compositions of rainfall ($\delta^{18}\text{O}_{\text{mw}}$) corrected from altitude (see
993 $\delta^{18}\text{O}_{\text{mw}}^{**}$ in Supplementary Table 5) are reported against the calendar ^{14}C dates (years

994 AD) measured on human bone collagen (Supplementary Table 2). The mean $\delta^{18}\text{O}_{\text{mw}}$
995 of -2.1 ± 1.5 (‰ VSMOW) recorded during the Medieval Warm Period (MWP) is
996 significantly higher than that of -4.4 ± 1.2 (‰ VSMOW) recorded during the Little Ice
997 Age (LIA). (see Supplementary Table 6 for statistical tests)

998

999 Figure 5: Carbon, nitrogen and sulfur isotope compositions of human bone collagen reported
1000 as a function of the ^{14}C -determined calendar dates AD (years). Note that the three
1001 isotopic ratios are significantly higher during the LIA than the MWP (see
1002 Supplementary Table 6 for statistical tests). Filled red squares represent mean values
1003 while error bars illustrate standard deviations.

1004

1005 Figure 6: $\delta^{15}\text{N}$ – $\delta^{13}\text{C}$ bivariate plot for the bone collagen of pre-Hispanic individuals from
1006 Gran Canaria. The positive correlation ($R = 0.5$; $n = 16$) suggests that a part of the
1007 variance is due to an increase in seafood consumption but also to an increase in water
1008 stress between the MWP and the LIA.

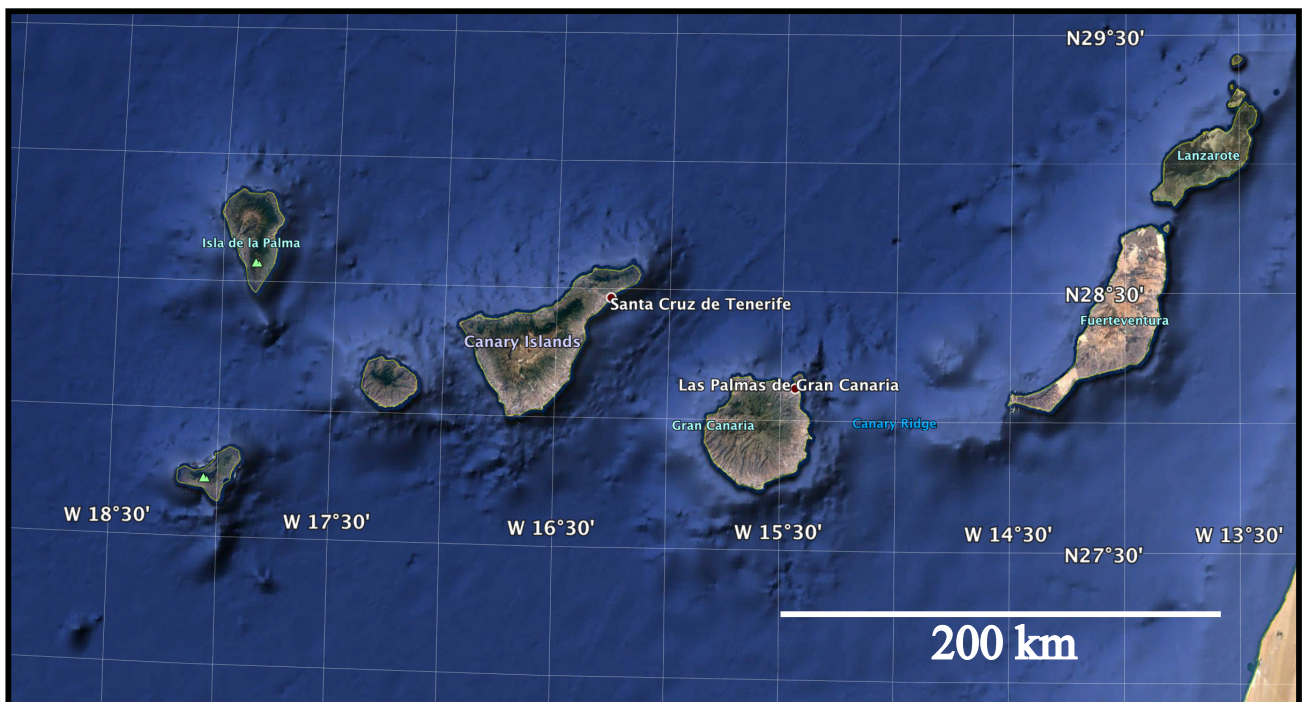
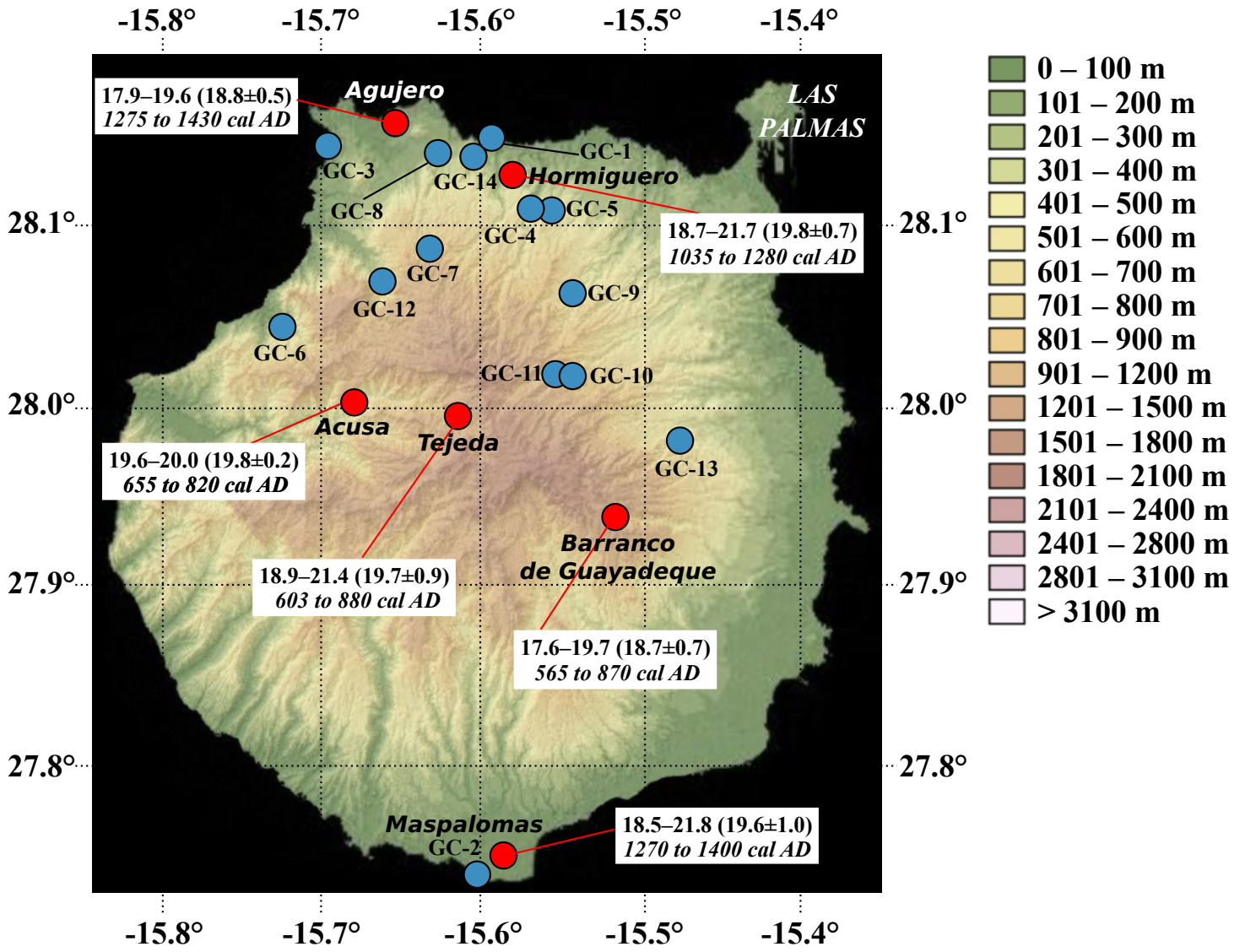
1009

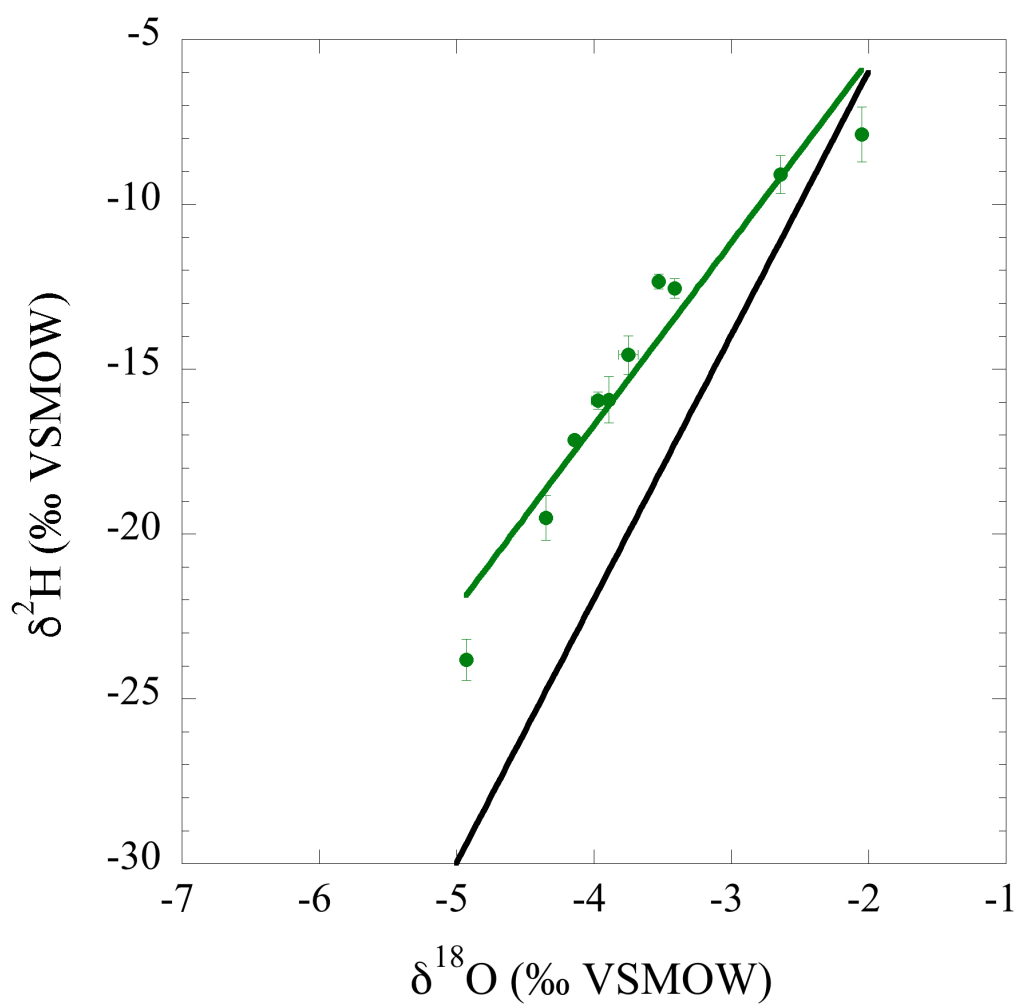
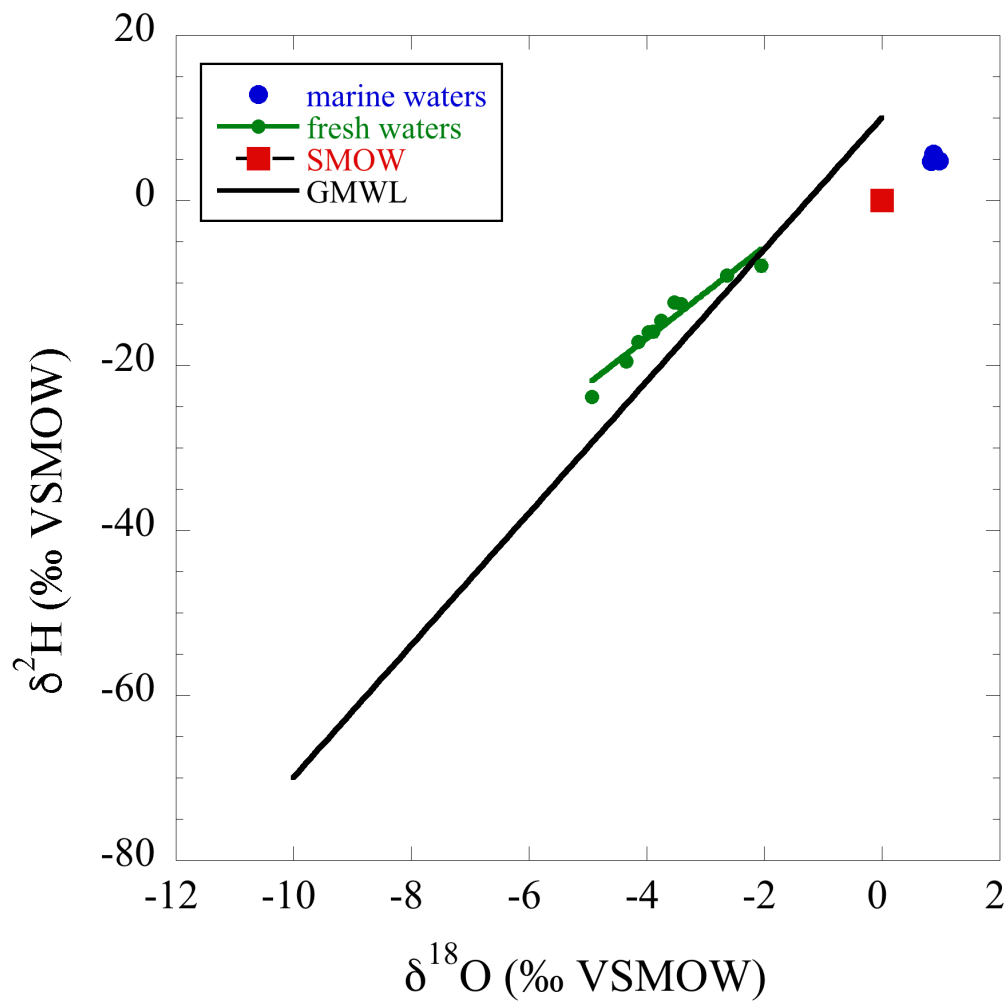
1010 Figure 7: $\delta^{15}\text{N}$ – $\delta^{34}\text{S}$ bivariate plot for the bone collagen of pre-Hispanic individuals from
1011 Gran Canaria. A) Linear fit performed with all data ($R = 0.45$; $n = 15$) and B) linear fit
1012 performed without the outlier ‘C4ind10’ ($R = 0.72$; $n = 14$). The positive correlation
1013 suggests that a part of the variance is due to an increase in seafood consumption
1014 between the MWP and the LIA.

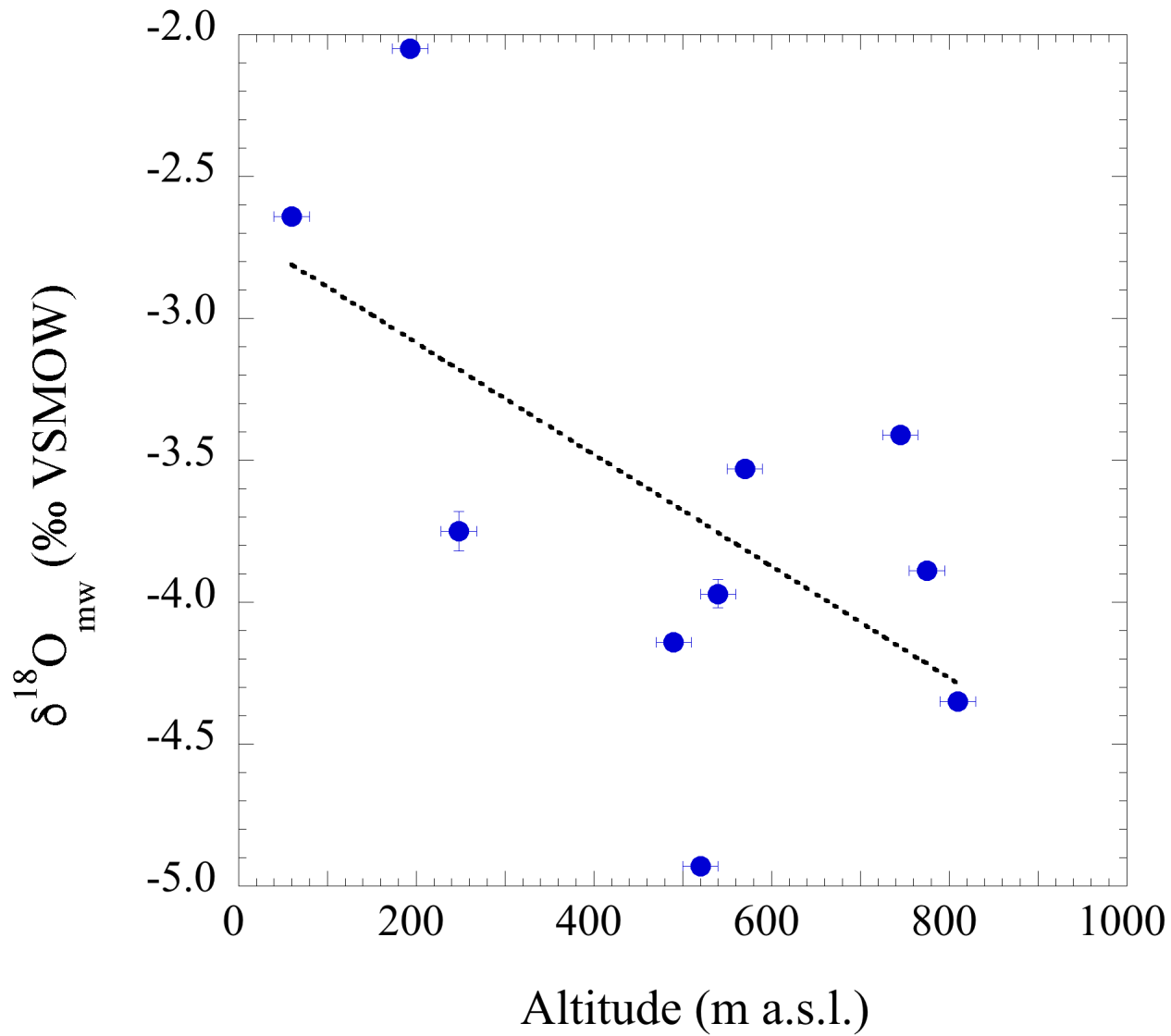
1015

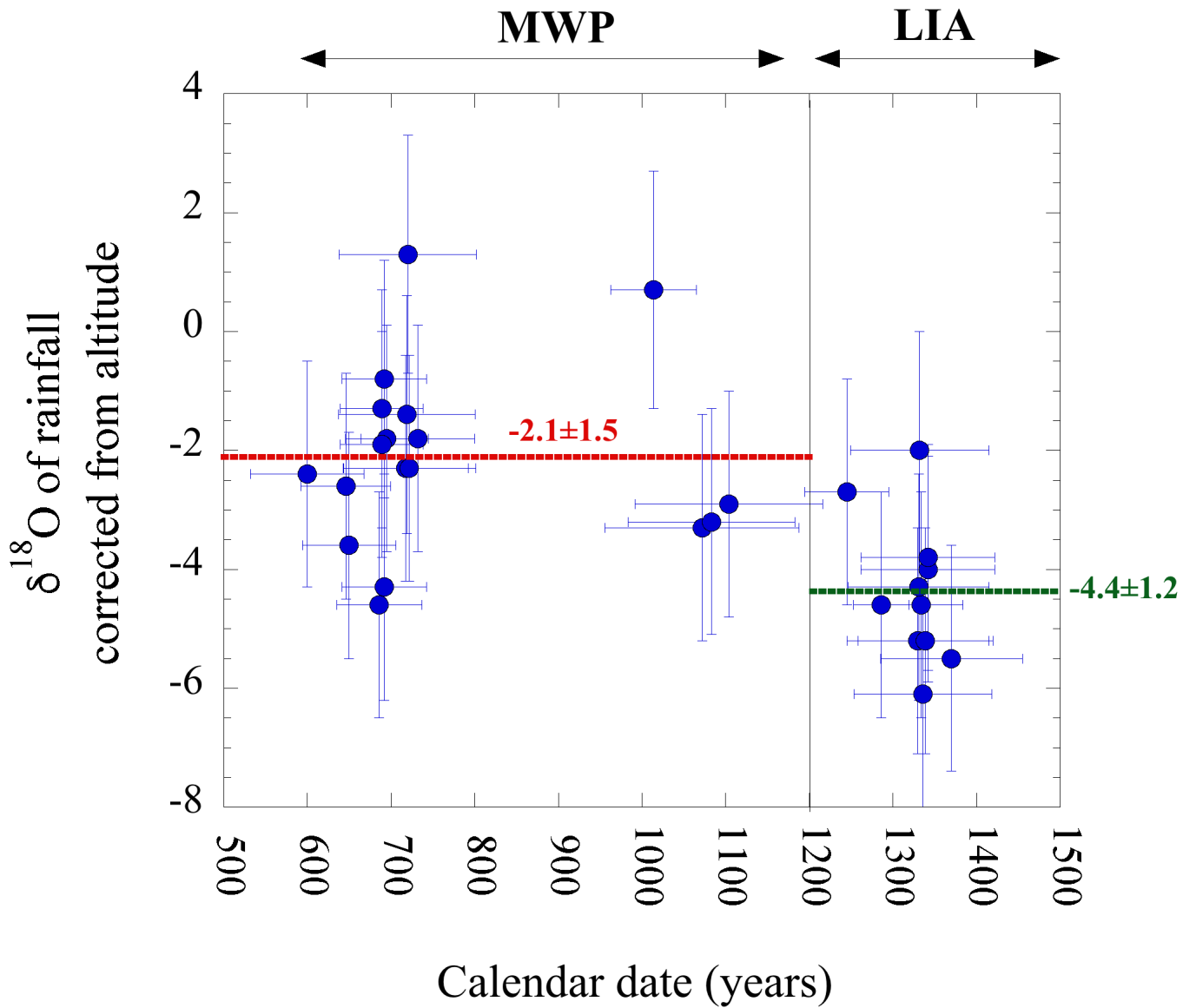
1016 Figure 8: A) Mean annual air temperature ($^{\circ}\text{C}$) reported against the altitude above sea level on
1017 the northern side of Gran Canaria. Error bars illustrate the mean range of variations for
1018 both variables. A linear fit of data defines a slope of -0.0044 ± 0.0004 and an intercept

1019 of -21.49 ± 0.44 ($R = -0.98$; $n = 5$). B) Monthly air temperature in Tenerife Island
1020 reported as a function of the $\delta^{18}\text{O}$ of meteoric waters (‰ VSMOW). Data come from
1021 the IAEA/WMO database. A linear fit of data defines a slope of 2.01 ± 0.22 and an
1022 intercept of 22.4 ± 0.43 ($R = 0.96$; $n = 9$). No data are available for July, August and
1023 September because of the absence of precipitations.

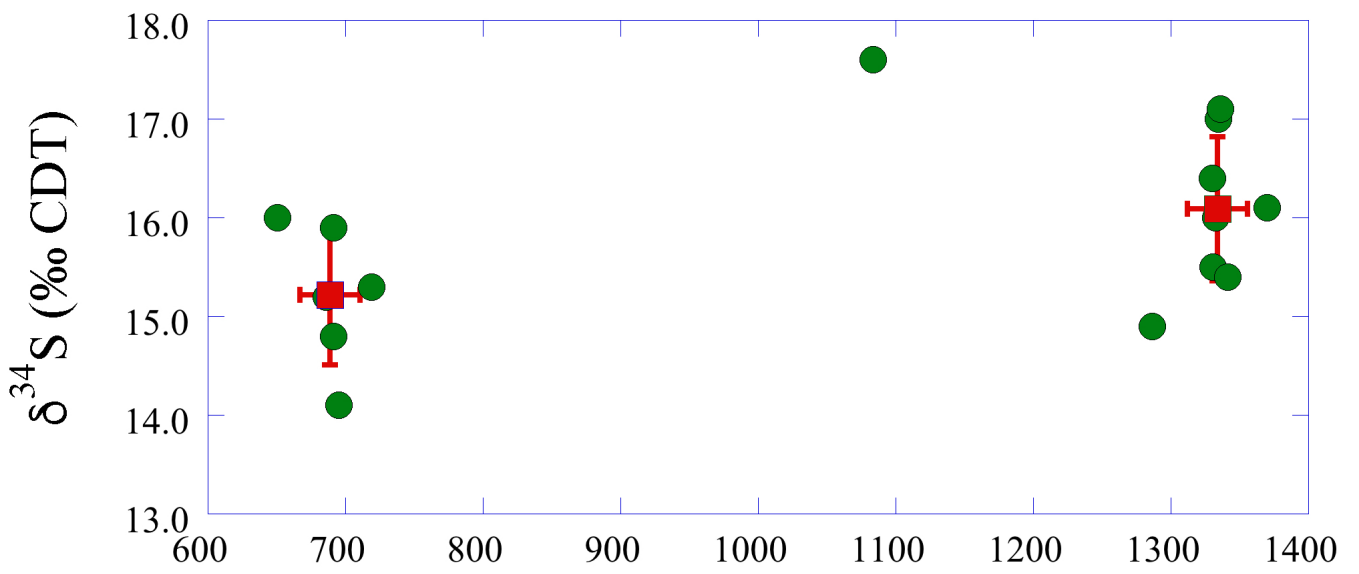
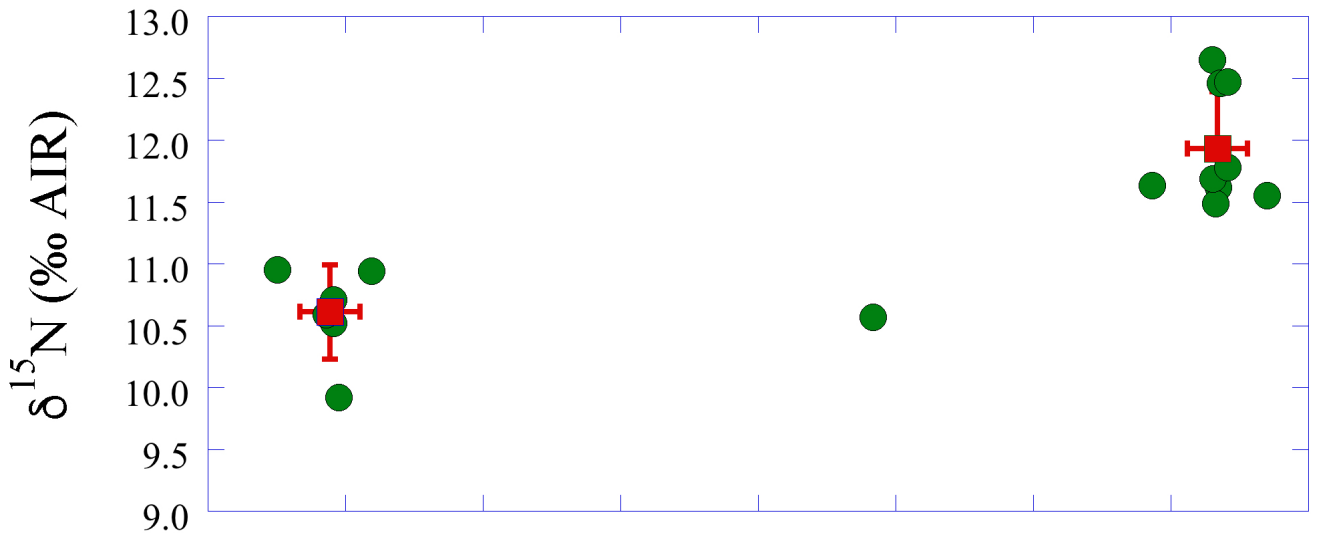
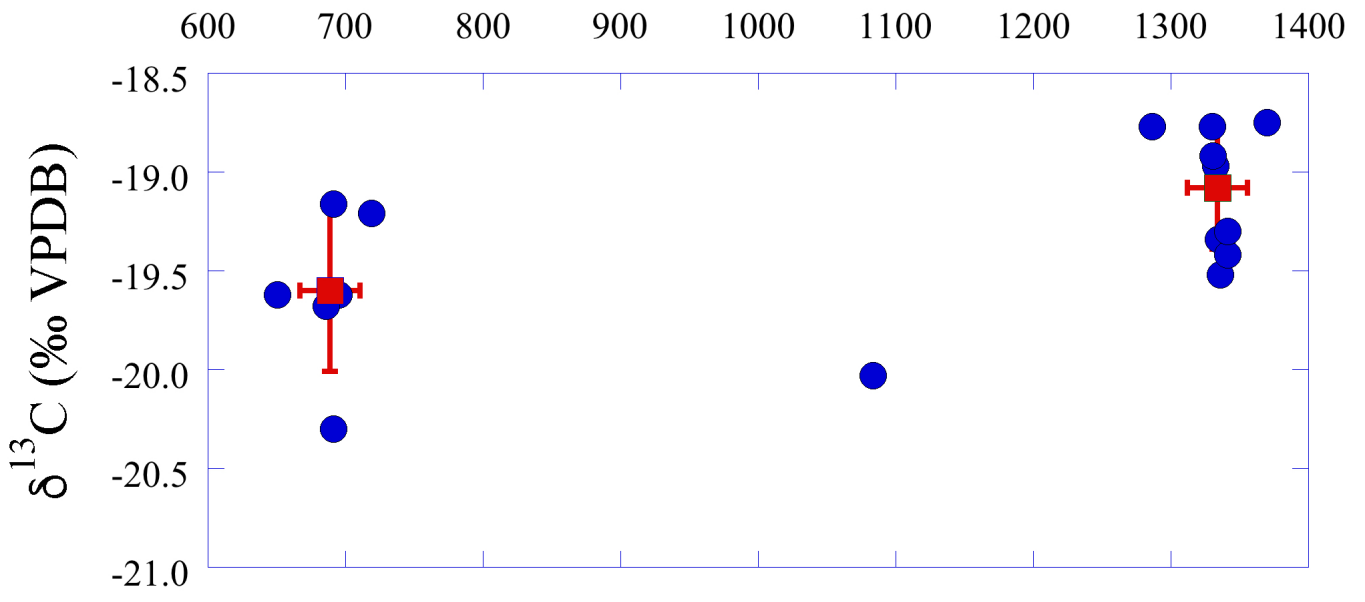




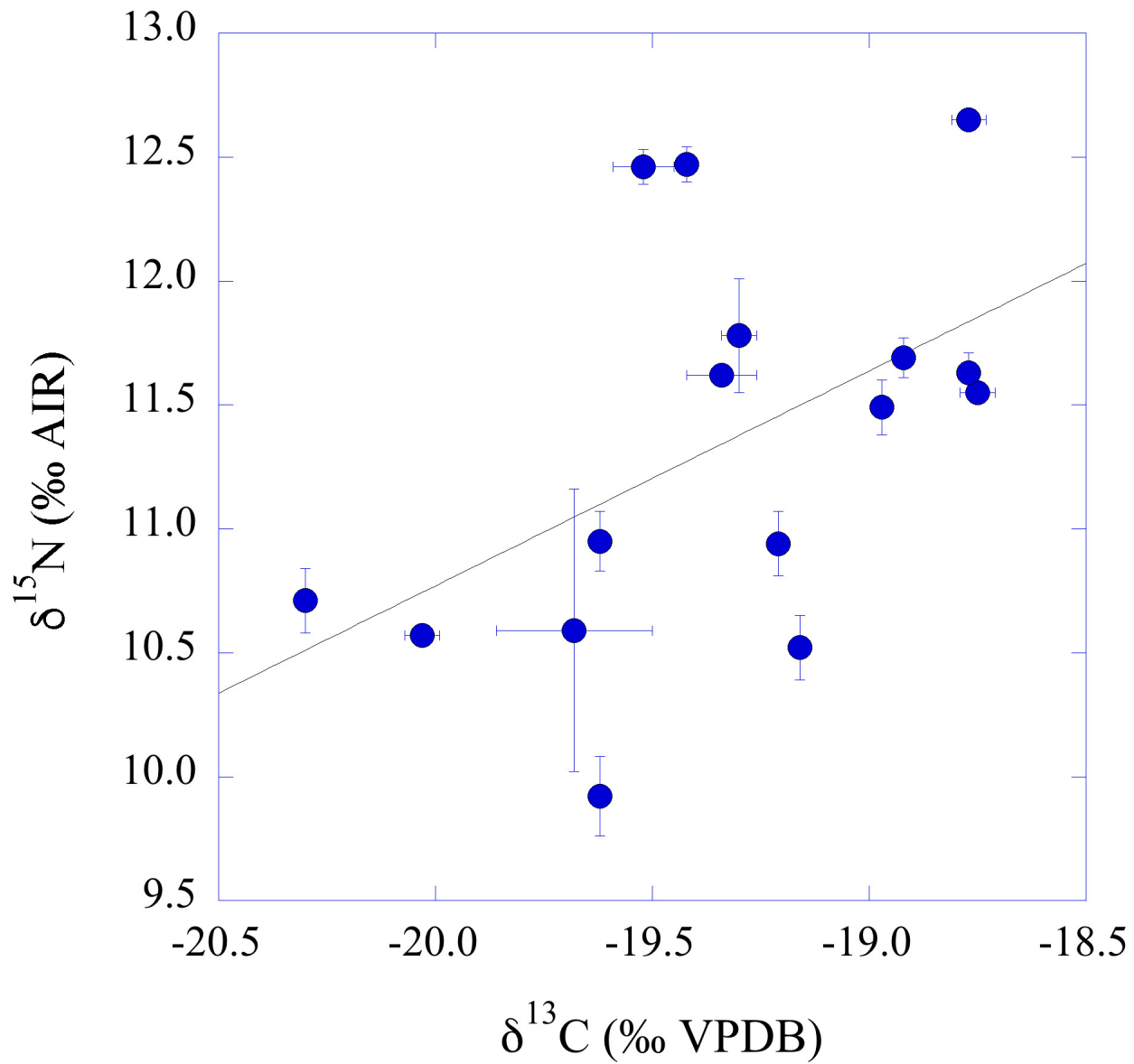




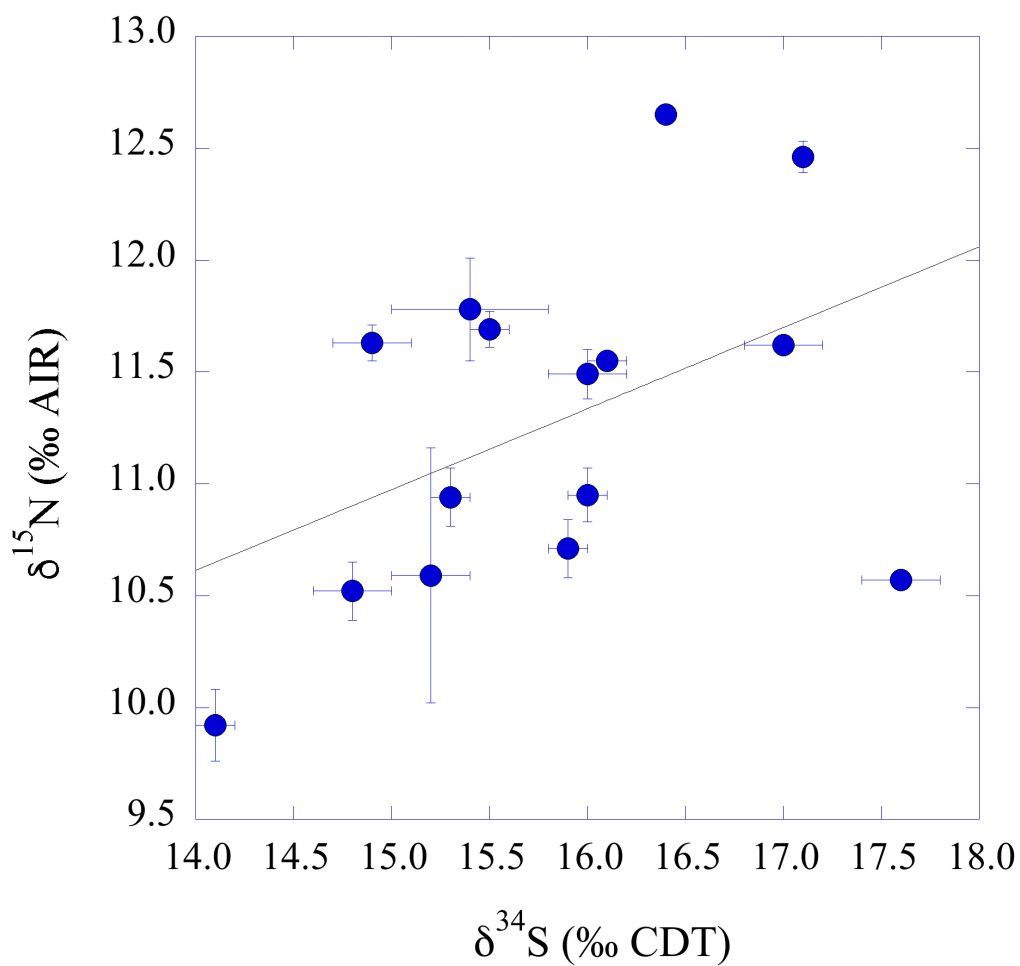
Calendar date



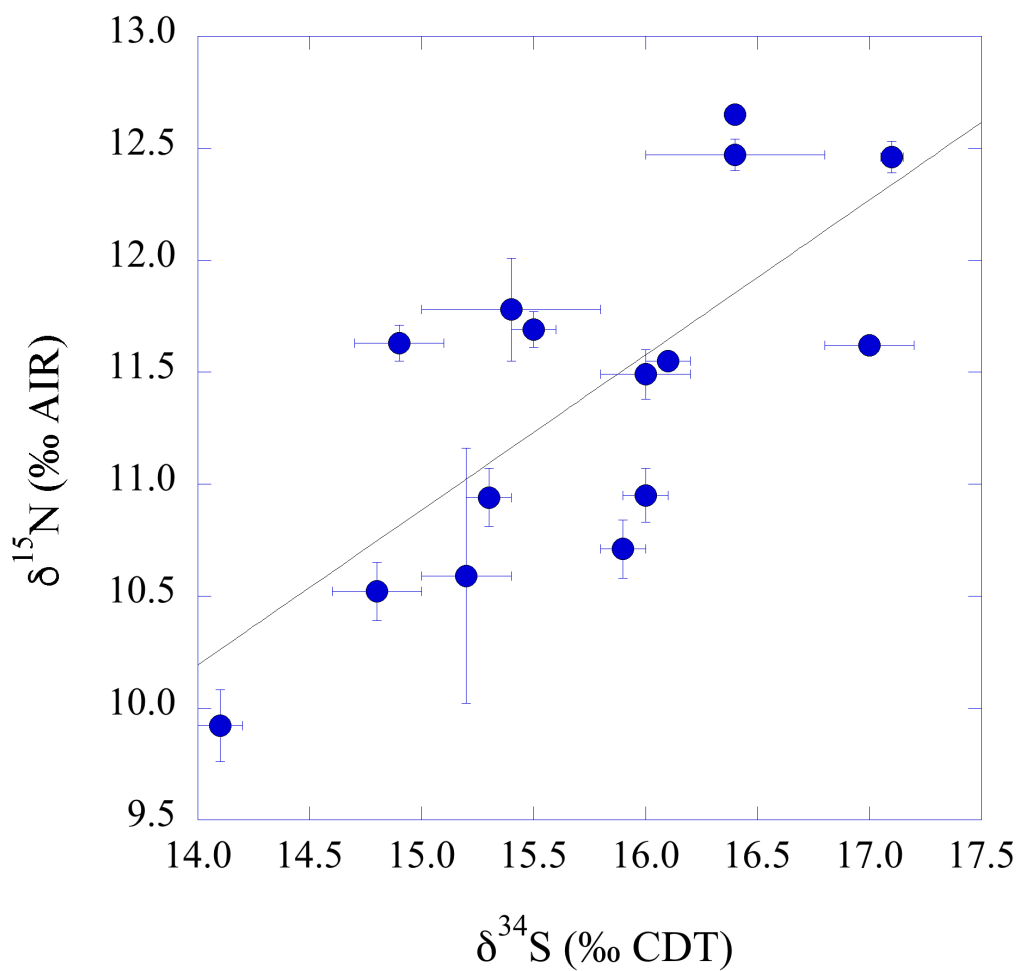
Calendar date



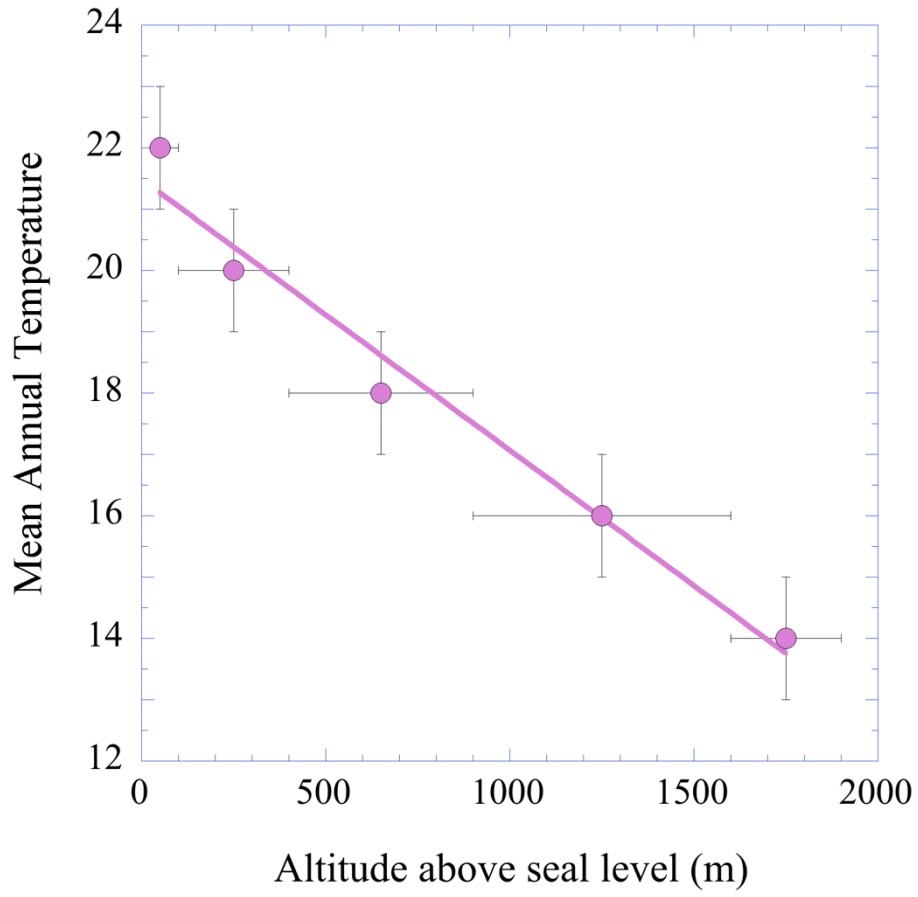
A)



B)



A)



B)

